N70 31601
N70- 31608
NASA CR 86394

COMMERCIAL AIR TRANSPORT HAZARD WARNING AND AVOIDANCE SYSTEM

(Final Report)

VOLUME III - RADAR PERFORMANCE STUDIES

By: T. G. Thorne
Polhemus Navigation Sciences, Inc.

CASE FILE
COPY

POLHEMUS NAVIGATION SCIENCES, INC.
P.O. BOX 1011; BURLINGTON, VERMONT 05401; PHONE 802/658-1450

PNSI-TR-70-0414-III

COMMERCIAL AIR TRANSPORT
HAZARD WARNING AND AVOIDANCE SYSTEM

(Final Report)

VOLUME III - RADAR PERFORMANCE STUDIES

By: T. G. Thorne
Polhemus Navigation Sciences, Inc.

May 1970

Prepared under Contract No: NAS 12-2108

by
POLHEMUS NAVIGATION SCIENCES, INC.
Burlington, Vermont
05401

for: Electronics Research Center
NATIONAL AERONAUTICS AND SPACE ADMINISTRATION

Mr. Harold Decker
Technical Monitor
NAS 12-2108
Electronics Research Center
575 Technology Square
Cambridge, Massachusetts 02139

"Requests for copies of this report should be referred to:

NASA Scientific and Technical Information Facility
P.O. Box 33, College Park, Maryland 20740"

PNSI-TR-70-0414-III

COMMERCIAL AIR TRANSPORT
HAZARD WARNING AND AVOIDANCE SYSTEM

(Final Report)

VOLUME III - RADAR PERFORMANCE STUDIES

By: T. G. Thorne
Polhemus Navigation Sciences, Inc.

May 1970

Prepared under Contract No: NAS 12-2108
by
POLHEMUS NAVIGATION SCIENCES, INC.
Burlington, Vermont
05401

for: Electronics Research Center
NATIONAL AERONAUTICS AND SPACE ADMINISTRATION

FOREWORD

The work described in this three volume report was performed by Polhemus Navigation Sciences, Inc., for the Electronics Research Center, Cambridge, Massachusetts, of the National Aeronautics and Space Administration, under Contract NAS - 12-2108. The study was oriented towards the development of a Commercial Air Transport Hazard Warning and Avoidance System with particular emphasis on alleviating the problem of aircraft all-weather landing. The NASA Technical Monitor for the Aircraft Hazard Avoidance Programs office during the initial phase of the study was Mr. Richard J. Miner. During the final portion of the study Mr. Harold Decker was the NASA Technical Monitor.

ABSTRACT

Analysis of the operational requirements for a Commercial Air Transport Hazard Warning and Avoidance System was performed in conjunction with a study of the available sensor technology suited to such a system. Particular emphasis was placed on the problem of low visibility landings through a comprehensive investigation into such factors as meteorological and visibility data, aircraft accident statistics, airline-related economic benefits, current and future landing aids, and present operating procedures. The technology study was concentrated primarily in the area of microwave sensors at frequencies in the X, Ka, Ku, and V bands, with some additional analysis of electro-optical and infra-red sensors. Operational requirements were studied for landings in visibility conditions down to and including Category IIIC.

Requirements for Independent Approach and Landing Monitor (IALM), High Ground Avoidance (HGA), and Roll-out and Taxi Aid (ROTA) functions were developed. Several possible system configurations were postulated as they applied to the overall operational and functional performance requirements.

Volume I of this report is a summary volume, containing an overview of the conclusions and recommendations of the study. The main body of the report, the operational requirements, technology analysis, and system analysis is contained in Volume II. Volume III is devoted to a detailed set of Radar Performance Studies which provide the technical background for the study.

TABLE OF CONTENTS

Foreword	iii
Abstract	v
Table of Contents	vii
List of Illustrations	ix
List of Tables	xi
Table of Symbols	xiii
Section	**Page**
1.0 INTRODUCTION	1
2.0 BACK SCATTERING FROM TERRAIN	4
2.1 Introduction	4
2.2 Scattering Coefficient	5
2.3 Surface Roughness	5
2.4 Grazing Angle	5
2.5 Polarization	6
2.6 Frequency	9
2.7 Seasonal and Meteorological Effects	9
2.8 Experimental Data	11
2.9 Conclusions	12
3.0 ATTENUATION OF RADAR SIGNALS BY WEATHER AND THE RESULTING EFFECTS ON RADAR PERFORMANCE	12
3.1 Introduction	12
3.2 Attenuation From Fog	15
3.3 Attenuation From Rain	16
3.4 Degradation of Radar Performance For Small Targets	16
3.5 Degradation of Radar Performance For Extended Targets	24
3.6 Conclusions	25
4.0 BACK SCATTER FROM RAIN	27
5.0 VISIBILITY OF RUNWAYS WITH A MAPPING RADAR	30
5.1 Introduction	30
5.2 Calculations	30

TABLE OF CONTENTS (cont'd)

Section		Page
6.0	SIGNAL LEVEL CALCULATIONS	37
6.1	Signal Reflected From Grassy Terrain	37
6.2	Receiver Noise	38
6.3	Signal Reflected From Rain	39
6.4	Signal Reflected From a Reflector	39
6.5	Ratio of Terrain Signal to Receiver Noise	40
6.6	Ratio of Terrain Signal to Rain Signal	43
6.7	Ratio of Reflector Signal to Receiver Noise	46
6.8	Ratio of Reflector Signal to Terrain Signal	50
6.9	Ratio of Reflector Signal to Rain Signal	51
6.10	Reflector Size for $S_c / S_t = 10dB$	52
6.11	Pulse Length and Reflector Size for S_c / N_r and S_c / S_t to be 10dB at a Given Range in 100 ft Visibility Fog	53
6.12	Beacon Power	59
6.13	Terrain Signal for a Pulse Width of 1 Microsecond	60
6.14	Rain Signal for a Pulse Width of 1 Microsecond	62
6.15	Comment	62
7.0	INTERFERENCE	63
7.1	Direct Interference	63
7.2	Reflected Interference	68
REFERENCES		70

LIST OF ILLUSTRATIONS

Figure		Page
III-1	Values of σ_o at Ka Band	7
III-2	Values at σ_o at Ku Band	7
III-3	Values of σ_o at Ka Band	8
III-4	Values of σ_o at Ku Band	8
III-5	Effects of Frequency Upon $\gamma$for 2 Inch Grass	10
III-6	Contrast of γ for various Smooth Surfaces at Ka Band	10
III-7	Contrast of γ for Various Smooth Surfaces at Ku Band	10
III-8	Contrast of γ for Various Smooth Surfaces at X Band	10
III-9	Effects of Rain on an Asphalt Road at Ka Band	10
III-10	Effects of Rain on 2 Inch Grass at Ka Band	10
III-11	Seasonal Changes of Grass at Ka Band	10
III-12	Oxygen Absorption	12
III-13a	Water Vapor Attenuation Factor	13
III-13b	Attenuation in Rain and Fog	14
III-14	Reduction in Range for Fog. (X-Band at 18°C)	17
III-15	Reduction in Range for Fog. (Ku-Band at 18°C)	18
III-16	Reduction in Range for Fog. (Ka-Band at 18°C)	18
III-17	Reduction in Range for Fog. (V-Band at 18°C)	19
III-18	Reduction in Range for 100 ft. Visibility Fog at 0°	20
III-19	Reduction in Range for Rain (X-Band at 18°C)	20
III-20	Reduction in Range for Rain Ku-Band at 18°C	21
III-21	Reduction in Range for Rain Ka-Band at 18°C	21
III-22	Reduction in Range for Rain V-Band at 18°C	22
III-23	Unattenuated Radar Range vs Radar Target Cross Section	23
III-24	Range in 100 ft. Fog on Grass	26
III-25	Theoretical Cross Section per Unit Volume for Various Rainfall Rates	28
III-26	Beam Intercept on Runway	31
III-27	Detection Range of 300 ft. Runway for Various Azimuth Beamwidths	35
III-28	Fall in Signal as Beam Sweeps Through 300 ft. Runway	35
III-29	Fall in Signal as Beam Sweeps Through 300 ft. Runway	36
III-30	Values of 3 [R] - 2 [ψ] for X Band	44
III-31	Values of 3 [R] - 2 [ψ] for Ku Band	44
III-32	Values of 3 [R] - 2 [ψ] for Ka Band	45
III-33	Values of 3 [R] - 2 [ψ] for V Band	45
III-34	4 [R] - 2 [ψ] for X Band	48

LIST OF ILLUSTRATIONS (contd.)

Figure		Page
III-35	4 [R] - 2 [ψ] for Ku Band	48
III-36	4 [R] - 2 [ψ] for Ka Band	49
III-37	4 [R] - 2 [ψ] for V Band	49
III-38	Values of 2 [R] - [ψ] for X Band	65
III-39	Values of 2 [R] - [ψ] for Ku Band	65
III-40	Values of 2 [R] - [ψ] for Ka Band	66
III-41	Values of 2 [R] - [ψ] for V Band	66
III-42	Reflected Interference	68

LIST OF TABLES

Table No.		Page
III-1	Grass/Concrete Scattering Coefficient Ratio	6
III-2	Location of Curves in Ohio State Terrain Handbook	11
III-3	Attenuation from Fog at 18°C	15
III-4	Attenuation from Fog at 0°C	15
III-5	Attenuation from Rain at 18°C	16
III-6	Typical Parameters of Radars	23
III-7	Theoretical Values of Radar Cross Section of Rain	29
III-8	Runway Detection Range	34
III-9	Detection Range of 300 ft. Runway with 10dB Grass/ Runway Ratio	34
III-10	Detection Range of 300 ft. Runway with 20dB Grass/ Runway Ratio	36
III-11	Radar Parameters	38
III-12	Values of 2 (ψ)	41
III-13	Range at Which Terrain Signal/Noise = 10dB	42
III-14	Range at Which Terrain Signal/Noise = 20dB	43
III-15	Range in km for Terrain Signal/Rain Signal = 10	46
III-16	Range on 1000m^2 Reflector, Signal/Noise = 10	50
III-17	Range at Which Reflector Signal/Terrain Signal = 10	51
III-18	Range at Which Reflector Signal/Rain Signal = 10	52
III-19	Size of Reflector to Give Sc/St of 10dB at a Range of 300m	53
III-20	Optimum Pulse Length and Minimum Reflector Size for X Band in 100 ft. Visibility Fog	54
III-21	Optimum Pulse Length and Minimum Reflector Size for Ku Band in 100 ft. Visibility Fog	55
III-22	Optimum Pulse Length and Minimum Reflector Size for Ku Band with 'Typical' Attenuation Assumed for 100 ft. Visibility Fog	55
III-23	Optimum Pulse Length and Minimum Reflector Size for Ka Band in 100 ft. Visibility Fog	57
III-24	Optimum Pulse Length and Minimum Reflector Size for Ka Band with 'Typical' Attenuation Assumed for 100 ft. Visibility Fog	57
III-25	Optimum Pulse Length and Minimum Reflector Size for V Band in 100 ft. Visibility Fog	58
III-26	Optimum Pulse Length and Minimum Reflector Size for V Band with 'Typical' Attenuation Assumed for 100 ft. Visibility Fog	58

LIST OF TABLES (contd)

Table No.		Page
III-27	Beacon Power for a 10dB Signal/Noise Ratio at 10nm	60
III-28	Terrain Signal Variation with Range	61
III-29	Rain Signal Variation with Range	62
III-30	Values of 2 R - ψ	64
III-31	Range at Which Direct Interference Signal is 10dB Above Receiver Noise. Side Lobe to Side Lobe Transmission	67
III-32	Range for Interference Signal to be 10dB Above Receiver Noise with the Ku Band Radar	68
III-33	Ratio of Reflected Interference to Terrain Signal	69

LIST OF SYMBOLS

. Arabic Letter Listing (lower case)

c	propagation velocity
p	partial pressure of water vapor (mm of mercury)
k	Boltzmann's constant
t	pulse width
w	runway width
x, y	variables of integration

. Arabic Letter Listing (caps)

B	receiver bandwidth
G	antenna gain
G_b	beacon antenna gain
G_1	antenna gain of the interfering radar in the direction of the interfered radar
G_2	antenna gain of the interfered radar in the direction of the interfering radar
H	absolute humidity
HP	horizontal polarization
VP	vertical polarization
K	a numerical constant
K_1	a factor which depends upon beamwidth and range
N	radar receiver noise figure
N_r	receiver noise
P	radar transmitter power
P_b	beacon transmitter power
P_n	noise power
R	range
R_d	range through dry air
R_w	range through wet air
S/N	signal-to-noise ratio
S	signal received
S_b	signal received from beacon
S_c	signal received from reflector
S_d	signal received through dry air
S_i	signal received, interference
S_r	signal received from rain
S_t	signal received from terrain
S_w	signal received through wet air
S_α	signal required for reliable detection
T	absolute temperature
V	volume in one-half pulse length

. Greek Letter Listing (lower case)

α	elevation beamwidth
α_ω	one-way attenuation factor for water droplets
β	azimuth beamwidth
β_ω	one-way attenuation factor for water vapor
γ	scattering coefficient
γ_a	attenuation constant
γ_1	scattering coefficient of terrain
γ_2	scattering coefficient of runway surface
θ	grazing angle
λ	wavelength
σ	effective radar cross section
σ_e	effective radar cross section of rain
σ_u	radar cross section of rain per unit volume
σ_o	terrain scattering property, $\gamma \sin \theta$
ψ	one-way attenuation term, Exp $(-K \gamma_a R)$
ψ_1	attenuation term for path R_1
ψ_2	attenuation term for path R_2

. Symbols

[ ]	enclosure of a variable in square brackets indicates its expression in decibels (dB)

COMMERCIAL AIR TRANSPORT

HAZARD WARNING AND AVOIDANCE SYSTEM

(Final Report)

VOLUME III - RADAR PERFORMANCE STUDIES

By: T. G. Thorne
Polhemus Navigation Sciences, Inc.
Burlington, Vermont 05401

1.0 INTRODUCTION

This volume of the report provides the background of radar performance analysis which is used in the discussions of Volume II. Radar performance is derived in terms of range capability which is obtained by establishing desired ratios of signal levels and calculating the ranges at which these criteria are satisfied. Throughout the volume, emphasis is placed upon deriving a realistic basis for illustrating the important characteristics of a radar sensor and for choosing among the available frequency bands at which a radar might be operated.

Both metric and British units are used in the work that follows. Metric units are used in most of the work because of the general trend of technical expression toward their use and because of the inherent convenience of their decimal nature. However, many users of the results are more accustomed to British units; therefore, results of the work, particularly in Volume II, are expressed in British units as well as metric.

The basic radar relationships used are fundamental equations such as

$$S = \frac{PG}{4\pi R^2} \cdot \frac{\sigma}{4\pi R^2} \cdot \frac{G\lambda^2}{4\pi} \qquad (1)$$

where: S = received signal (watts)
P = transmitted power (watts)
G = antenna gain
λ = wavelength (meters)
σ = effective radar cross section (square meters) and
R = range (meters)

The previous equation describes the signal return in the case where the effective cross section of the radar target is small in relation to the cross section of the radar beam. The current application requires consideration of radar signals from extended area targets

such as terrain, and volume targets such as rain. When the radar is looking obliquely down at terrain, the effective area of the target is

$$\sigma = \gamma R \beta \frac{ct}{2} \tan \theta \qquad (2)$$

where: γ = scattering coefficient
β = azimuth beamwidth (radians)
c = propagation velocity (meters per second)
t = pulse width (seconds) and
θ = grazing angle (degrees)

Beamwidth is the beamwidth between 3dB points.

For volume targets which fill the cross section of the beam, the effective area is

$$\sigma = \sigma_u V \qquad (3)$$

where: σ_u = radar cross section per unit volume and
V = volume in one-half pulse length

The volume in one-half pulse length is then given by

$$V = \frac{ct}{2} R \alpha R \beta. \qquad (4)$$

Considerable importance is also placed upon the attenuation which is caused by rain, fog, etc., along the propagation path. Attenuation is included in the form of an attenuation term. For example, when the attenuation term is included in Equation 1, the signal becomes

$$S = \frac{PG^2 \lambda^2 \sigma}{(4\pi)^3 R^4} \psi^2 \qquad (5)$$

where: ψ is the one-way attenuation term; and, therefore,

ψ^2 is the two-way attenuation term

The attenuation term is further defined by

$$\psi = \text{Exp}\,(-K\gamma_a R) \qquad (6)$$

where: γ_a = an attenuation constant, and

K = a numerical constant, 0.23026

In much of the report two-way attenuation is used. It is implemented by using the one-way attenuation constant and a numerical constant of

$$2K = 0.461$$

These equations are appropriately combined and evaluated in the sections that follow. They are applied to study radar performance at the following frequencies.

band	frequency
X	10 GHz
Ku*	16 GHz
Ka*	35 GHz
V	70 GHz

Radar performance is derived in terms of range capability. The range capability is obtained by establishing desired ratios of signal levels and calculating the ranges at which these criteria are satisfied.

*It would be more precise to subscript the a and the u modifiers for K band. The notation used here is simpler and, it is believed, conveys the message nearly as well.

2.0 BACK SCATTERING FROM TERRAIN

2.1 Introduction

The difference in the radar returns at low grazing angles from a runway and the adjacent terrain determines whether an Independent Approach and Landing Monitor radar (IALM) can of itself locate the runway, or whether enhancement techniques are required.

When terrain is illuminated by a pulse radar, the signal power received at the radar receiver is given, from equations 1 and 2, by:

$$S_t = \frac{PG^2\lambda^2}{(4\pi)^3 R^3} \gamma\beta \frac{ct}{2} \tan\theta \qquad (7)$$

where:

S_t = received signal (watts)

P = transmitter power (watts)

G = antenna gain

λ = wavelength (meters)

c = velocity of propagation (meters per second)

t = pulse width (seconds)

β = azimuth beamwidth (radians)

θ = grazing angle (degrees)

γ = scattering coefficient

R = range (meters)

In equations 2 & 7, the scattering coefficient, γ, relates to an equivalent area which is normal to the radar beam. An alternative method of expression is to use the true ground area illuminated by the radar and a modified scattering coefficient given by:

$$\sigma_o = \gamma \sin\theta$$

2.2 Scattering Coefficient

The fundamental parameters that affect the magnitude of the scattering coefficient are:

- Surface roughness.
- Grazing angle.
- Complex dielectric constant of the terrain.
- Polarization of the radar signal.
- Frequency of the radar signal.

The only parameters that can be controlled by the equipment designer are the type of polarization and the transmitter frequency. But, as shown in other sections of this report, the choice of frequency and type of polarization are also affected by other considerations.

Although there appears to be little information on the scattering coefficients at grazing angles below 10°, there is considerable information available for angles greater than 10°. Probably the most comprehensive source of this information is the Ohio State University Terrain Handbook (Ref. 1).

2.3 Surface Roughness

Surface roughness usually has a very important effect upon the terrain return but the effect may be reduced at low grazing angles. Generally, it is convenient to divide surfaces into two classes, "rough" and "smooth", in order to predict the effect of other parameters on the return from terrain. A surface is defined as "smooth" if it has a continuous structure with a root mean square surface roughness much less than a wavelength. A surface is "rough" if its root mean square variation is many wavelengths. The surfaces which are considered here probably fall between the two classes described above, but it is instructive to consider "rough" and "smooth" surfaces when discussing effects of other parameters.

2.4 Grazing Angle

As indicated above, the grazing angle is closely constrained to typical aircraft approach angles and is not a parameter that is available for optimization in the IALM system. It does have important implications on system design, however, because very little surface scattering data is available down to grazing angles of 3°. For surfaces that

are truly smooth, γ generally increases with the grazing angle, and for X and Ku band signals it is probably safe to extrapolate from 10° to 3°. For surfaces that are truly rough, γ is generally independent of grazing angle and it should be safe to extrapolate from 10° to 3°. For surfaces which are in between, e.g. concrete or asphalt runway, extrapolation at Ka band may not give accurate information. It is known that there is a minimum value of γ for many such surfaces at an angle of about 5° (depending on the surface) and a sharp increase in γ below this angle. This might be expected with vertical polarization because of the Brewster angle effect but it has also been observed in the case of horizontal polarization (Ref. 2 and 3). Thus, the extrapolation from 10° to 3° is probably not reliable for such surfaces at Ka band.

2.5 Polarization

For smooth surfaces such as concrete, the Terrain Handbook shows that the magnitude of γ is less for horizontal polarization than for vertical at low grazing angles. This is indicated from curves I and J of Figure III-1 and Curves A and B of Figure III-2. It is also shown to be true for 4" snow in Figure III-4. One would expect that there would be less difference between the values of γ for different polarizations for rough surfaces, such as grass, than for smooth surfaces. This is true for Ka band, as indicated by curves K and L of Figure III-1, but it is not true for the Ku band curves C and D of Figure III-2. It is not clear why these unexpected results were obtained. The following differences in γ occur between green grass and concrete at a grazing angle of 10°.

TABLE III-1. GRASS/CONCRETE SCATTERING COEFFICIENT RATIO

Frequency Band	Polarization	Grass/Concrete Ratio dB	Derived From	Curves
Ka	Horizontal	21	Fig. III-1	L&J
Ka	Vertical	14	Fig. III-1	K&I
Ku	Horizontal	18	Fig. III-2	B&D
Ku	Vertical	20	Fig. III-2	H&C

In spite of the curves of Figure III-2, experience indicates that a better contrast should be obtained with horizontal polarization at Ku band. It is not clear whether this would also be the case at 3° incidence angle.

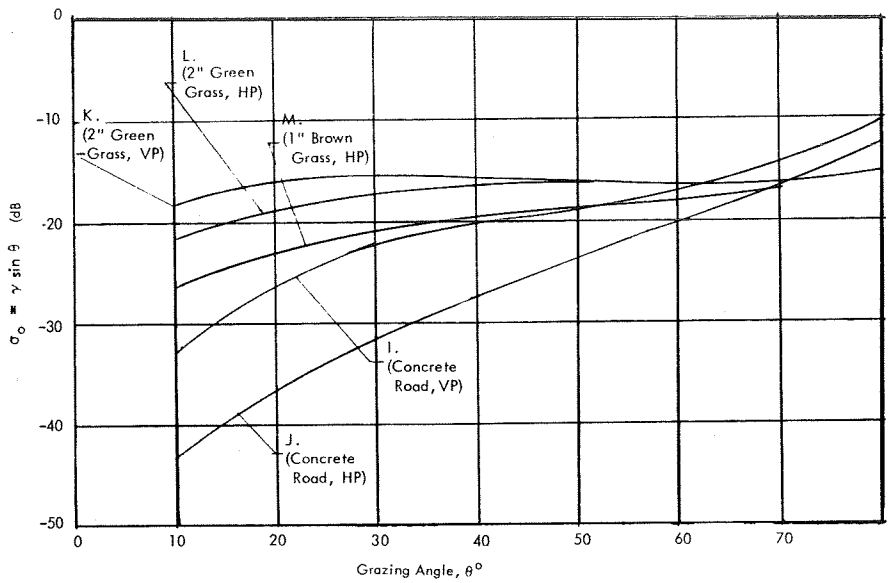

Figure III-1. Values of σ_o at Ka band.

VP - Vertical Polarization
HP - Horizontal Polarization

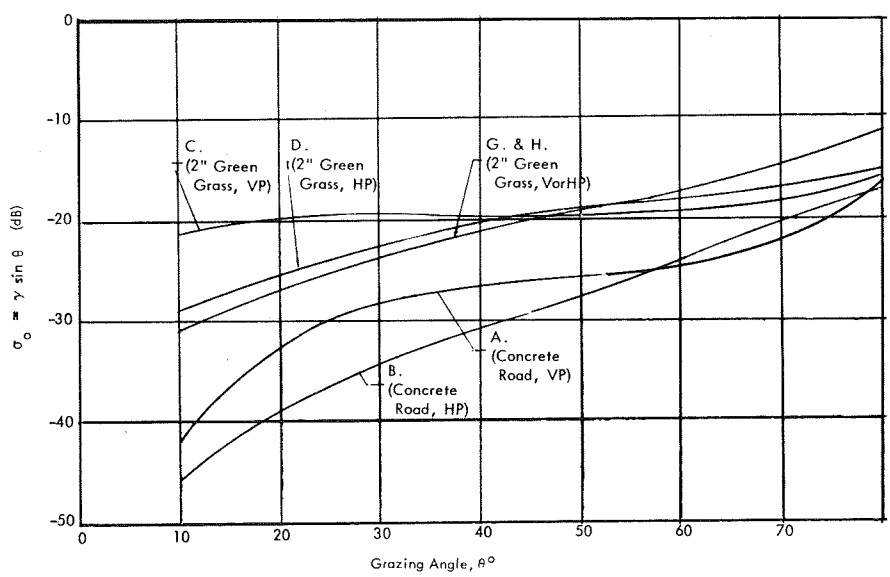

Figure III-2. Values of σ_o at Ku band.

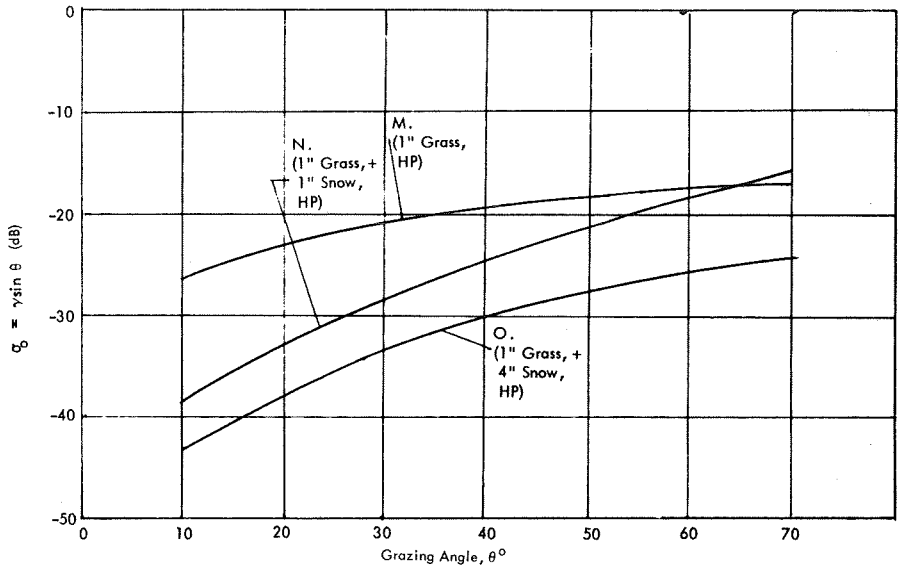

Figure III-3. Values of σ_o at Ka band.

VP - Vertical Polarization
HP Horizontal Polarization

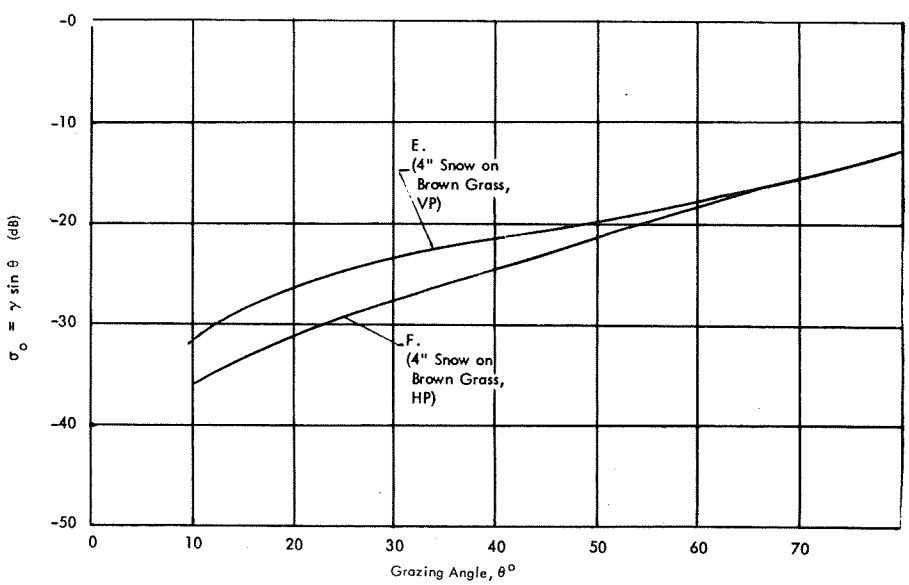

Figure III-4. Values of σ_o at Ku band.

2.6 Frequency

In general, the smoother the surface in relation to radar wavelength, the smaller the value of γ at low grazing angles. Thus, for concrete, one would expect γ to be greater at Ku band than at X band and, similarly, greater at Ka band than at Ku band. The same is true with rough surfaces, such as grass, only the change with frequency is not so great. Thus, there should be greater contrast at X band than at Ku band, and at Ku than at Ka band. Consider, for example, Figures III-5,6,7 and 8. At $\theta = 20^{\circ}$, the difference in γ between 2" grass and concrete is about:

12dB at X band (Figures III-5 & III-8)

11dB at Ku band (Figures III-5 & III-7)

8dB at Ka band (Figures III-5 & III-6)

Thus, the statements given above seem to be verified by the curves. Hence, if all other factors were equal, one would choose X band frequencies to improve the contrast between concrete runways and the adjoining grass strips. However, it is not definite whether these differences can be validly extrapolated to grazing angles as small as 3°.

2.7 Seasonal and Meteorological Effects

Figure III-9 shows that the value γ for a wet asphalt road at Ka band is much lower than when the road is dry. This decrease is due to the fact that the surface is smoothed by the water, and the complex dielectric constant (reflectivity) of the surface is changed by the water. Figure III-10 shows that the value of γ for grass at Ka band increases after rain. This is due to a change in the complex dielectric constant in the surface. In this case, the contrast is improved by rain, but the main point to be noted here is that there can be very significant changes in the value of γ when weather conditions change.

Seasonal changes in γ occur too. Consider Figure III-11 which shows how the value of γ changes during a year. At Ka band the change in γ is about 8dB. The seasonal problems are further illustrated by curves M of Figure III-1 and G & H of Figure III-2 which give the value of γ for brown grass at Ka and Ku bands. From these curves one can expect the contrast between grass and concrete to decrease from 3 to 10dB when the grass changes from green to brown. The problem is further aggravated if the ground becomes bare of grass and baked, as happens in some locations. In this case, the contrast would be almost nil. Figures III-2 and III-3 indicate that snow on the grass will also decrease the contrast between the runway and adjacent terrain. The value of γ for snow is difficult to predict since it depends on the depth of the snow, the wetness of the snow, and the smoothness of the snow crust. However, as an example of what could happen, consider the

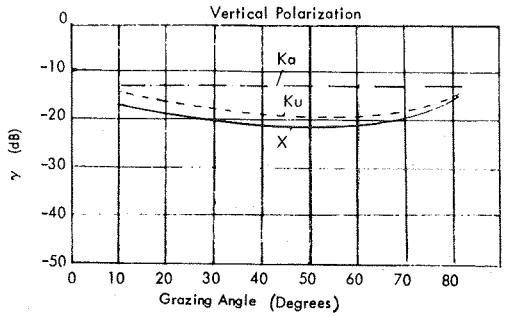

Figure III-5. Effects of Frequency Upon γ for 2 Inch Grass.

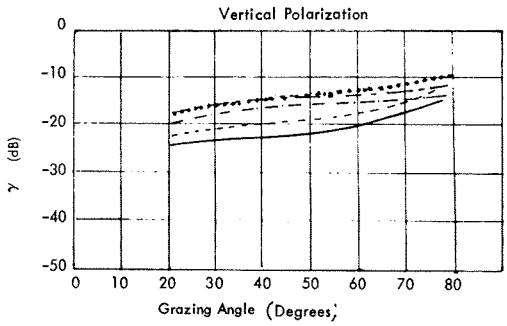

Figure III-6. Contrast of γ for various Smooth Surfaces at Ka band.

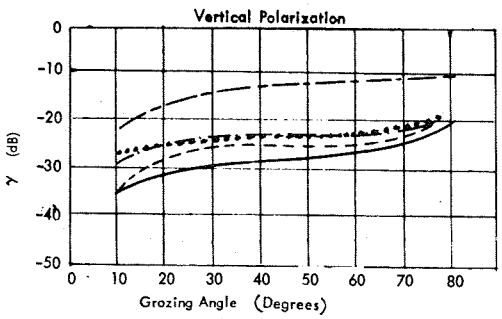

Figure III-7. Contrast of γ for Various Smooth Surfaces at Ku band.

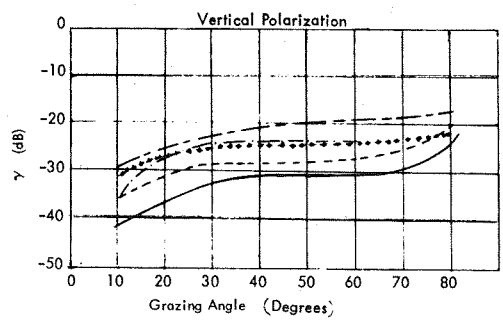

Figure III-8. Contrast of γ for Various Smooth Surfaces at X band.

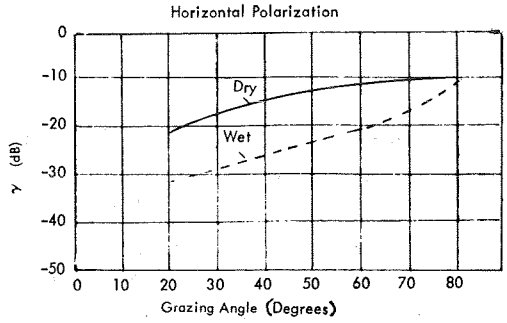

Figure III-9. Effects of Rain on an Asphalt Road at Ka band.

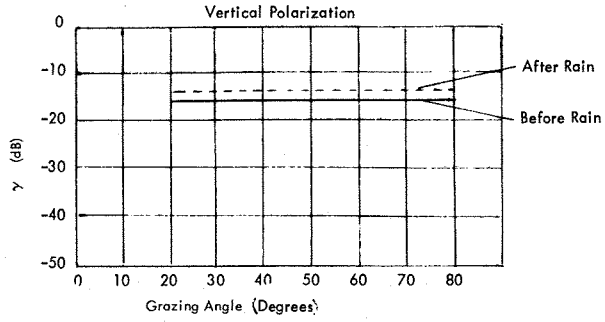

Figure III-10. Effects of Rain on 2 Inch Grass at Ka band.

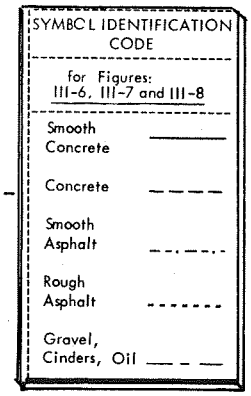

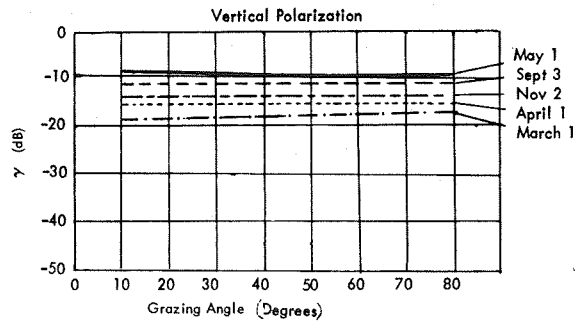

Figure III-11. Seasonal Changes of Grass at Ka band.

following case. Suppose there was horizontal polarization at Ka band with 4" of snow on 1" of grass and a bare concrete runway. Then at 10° grazing angle, the difference in γ between the snow and runway is about 0dB (curve J of Figure III-1 and curve O of Figure III-3). Thus, if this situation prevails, there will be no contrast between the runway and the snow.

2.8 Experimental Data

There appears to be very little experimental data at grazing angles below 10°. The sources of information for this Section come from the Ohio State Terrain Handbook (Ref. 1) from which Figures III-1 to 4 are taken (Table III-2 indicates where the curves are located in this book) and Figures III-5 through 11 come from Taylor's work (Ref. 4). Neither of these sources report data down to grazing angles of 3°, which are of interest in this program. No data is reported for V band and at this wavelength most runways will appear rough and they will probably afford very little contrast. However, this data should be obtained for completeness.

TABLE III-2 LOCATION OF CURVES IN OHIO STATE TERRAIN HANDBOOK (Ref.1)

Curve	Figure
A	5A - 13B
B	5A - 14B
C	5C - 1B
D	5C - 2B
E	5D - 10A
F	5D - 12B
G	5D - 8A
H	5D - 10B
I	5A - 13A
J	5A - 14A
K	5C - 1A
L	5C - 2A
M	5D - 2A
N	5D - 2B
O	5D - 2C

2.9 Conclusions

If there were no other considerations, one would attempt to maximize the contrast between runway and adjacent terrain by using X band with horizontal polarization. However, even if this were done, there are certain times of the year when the contrast would not be adequate. Hence, some type of enhancement will be necessary in order to be absolutely sure of detecting a runway.

3.0 ATTENUATION OF RADAR SIGNALS BY WEATHER AND THE RESULTING EFFECTS ON RADAR PERFORMANCE

3.1 Introduction

This section considers the attenuation of radar signals by water vapor and water droplets. The attenuation due to oxygen absorption is not included in the following discussion. The oxygen absorption can cause appreciable attenuation as shown in Figure III-12. However, by assuming a Ka band frequency of 35 GHz and a V band frequency of 70 GHz, it is reasoned that oxygen absorption will not be a key factor in selecting a desirable operating band for a radar sensor.

Let the power in the signal received by the radar from a given target at range R be given by S_r. Then for this same target and range, the power in the signal received when attenuation is present is

$$S_r \mathrm{Exp}\ (-2K\gamma_a R)$$

where γ_a is an attenuation constant, and

$2K$ is a numerical constant.

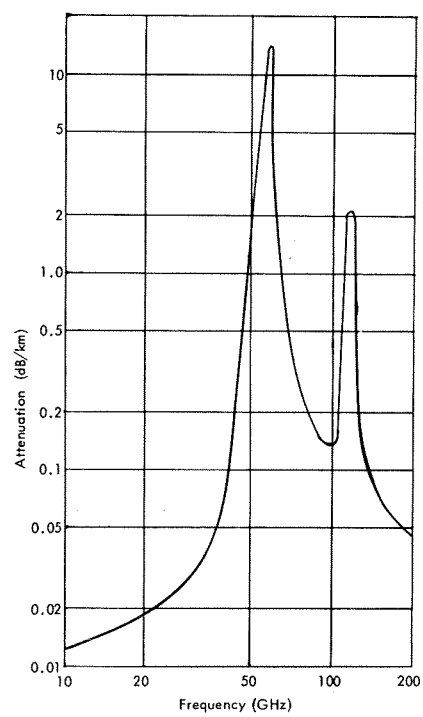

Figure III-12. Oxygen Absorption

γ_a is given in dB/km (one way). For this convention R is given in kilometers and 2K has the value 0.461.

Omitting the attenuation of oxygen, γ_a may be expressed as

$$\gamma_a = H\beta_\omega + \alpha_\omega$$

where H = absolute humidity (grams/meter^3)

β_ω = one-way attenuation factor for water vapor (dB/km)/(gram/m^3)

α_ω = one-way attenuation factor for water droplets (dB/km)

β_ω is a function of frequency and is shown in Figure III-13a. (This figure is adapted from one by Kerr, Ref. 5).

α_ω is a function of frequency, temperature, and meteorological conditions. The theoretical values of α_ω for four rain rates and three densities of fog are shown in Figure III-13b. (This curve was also taken from Kerr, Ref. 5). Thus for a given temperature, $\gamma_a = H\beta_\omega + \alpha_\omega$ is a function only of the meteorological condition and the frequency of the radar signal.

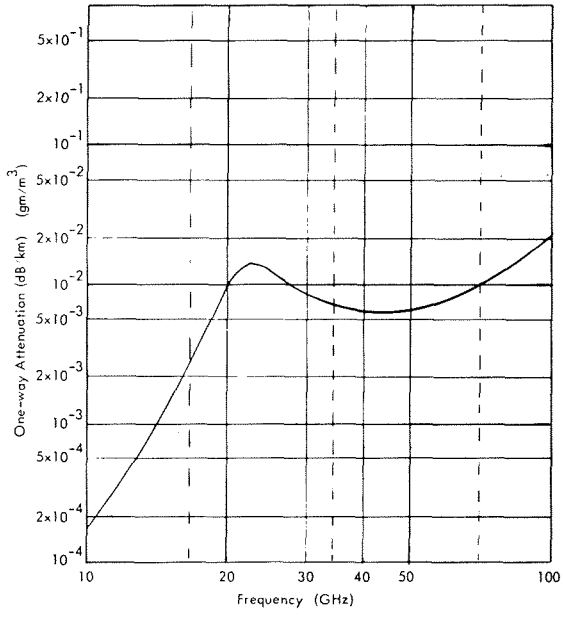

Figure III-13a. Water Vapor Attenuation Factor

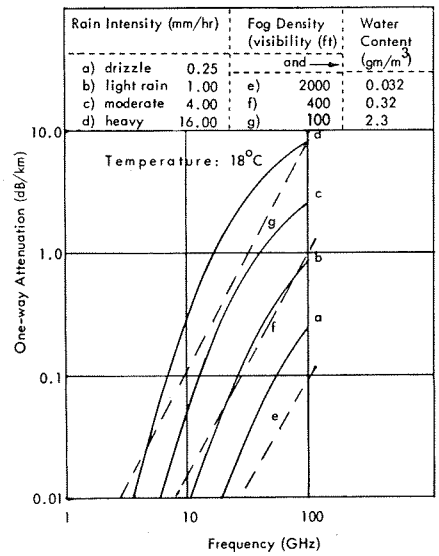

Figure III-13b. Attenuation in Rain and Fog

It should be noted that the experimental evidence collected so far indicates that the theoretical values of α_ω may be lower than the actual values. See Medhurst (Ref. 6) for a discussion of this point and a summary of the important experimental work in this area. Although the theoretical values may be slightly low, they will be used in this report since it is difficult to justify using any one given set of experimental data.

To specify γ_a , H must be obtained. The absolute humidity H is given by

$$H = \frac{288p}{T}$$

where p = partial pressure of water vapor in mm mercury

T = absolute temperature = 273+ °C

The vapor pressure of water at standard pressure is about 15.5 mm Hg at 18°C and is 4.58 mm Hg at 0°C. If a relative humidity is assumed, the relationship between partial pressure and vapor pressure is fixed and H can be specified for 18°C and 0°C, given the relative humidity.

3.2 Attenuation From Fog

Assuming that the relative humidity is 100%, the value of H is 15.35 grams/m^3 at 18°C. From the values of α_ω and β_ω given in Figure III-13, the values of $\gamma_a = H\beta_\omega + \alpha_\omega$ have been calculated and are listed in Table III-3 for the four frequencies of interest and three fog conditions.

TABLE III-3. ATTENUATION FROM FOG AT 18°C (dB/km, one way)

Fog Visibility	Frequency Band			
	X	Ku	Ka	V
2000 ft.			0.11	0.18
400 ft.	0.02	0.08	0.27	0.72
100 ft.	0.10	0.36	1.39	5.12

Temperature also has an effect on the attenuation from fog. Suppose a 100 ft. visibility fog occurs at 0°C. At this temperature, H = 4.83 grams/m^3 at 100% relative humidity. Furthermore, at 0°C the value of α_ω is increased over its value at 18° by a factor ranging from 2 at X band to 1.55 at V band (cf, Kerr, Ref. 5, p. 677). The value of γ_a for a fog of 100 ft visibility at 0°C are given in Table III-4. While fog at 0°C has a greater attenuation, fog at 18°C is judged to be a more typical occurrence and will be used in further analysis.

TABLE III-4. ATTENUATION FROM FOG AT 0°C (dB/km, one way)

Fog Visibility	Frequency Band			
	X	Ku	Ka	V
100 ft.	0.2	0.61	2.3	7.8

3.3 Attenuation From Rain

Table III-5 lists the calculated attenuation values from rain at a temperature of 18°C and a relative humidity of 80%. Values for α_ω and β_ω have been obtained from Figure III-13.

TABLE III-5. ATTENUATION FROM RAIN AT 18°C (dB/km, one way)

Rainfall (mm/hr)	Frequency Band			
	X	Ku	Ka	V
0.25		0.04	0.13	0.28
1.00	0.012	0.07	0.30	0.80
4.00	0.05	0.25	1.07	2.40
16.00	0.26	1.28	4.07	7.30

3.4 Degradation of Radar Performance for Small Targets

Consider how these attenuations degrade the radar performance using a technique adapted from Hawkins and LaPlant (Ref. 7). The following assumptions are made.

1. The atmosphere between the radar and target is uniform.
2. The target size is small compared to the cross section of the radar beam.
3. The attenuation of oxygen is omitted.

In a dry atmosphere the radar signal to noise ratio is:

$$S/N = S_d/P_n$$

and when rain or fog is present (neglecting back scatter from rain)

$$S/N = S_w/P_n$$

where P_n = noise power

S_d = signal power in dry air

S_w = signal power in wet air

Assuming the same signal to noise ratio is required for signal detection in wet air as in dry, then

$$S_d = S_w$$

From the radar equations

$$S_d = \frac{PG^2\lambda^2\sigma}{(4\pi)^3 (R_d)^4}$$

$$S_w = \frac{PG^2\lambda^2\sigma}{(4\pi)^3(R_w)^4} \quad \text{Exp}\ (-2K\gamma_a R_w)$$

hence $$R_d^4 = R_w^4 \ \text{Exp}\ (K\gamma_a R_w) \qquad (8)$$

where R_d = range in dry air (kilometers)

R_w = range in wet air (kilometers)

$2K = 0.461$

γ_a = attenuation constant (dB/km, one-way)

Unfortunately, one cannot solve Equation 8 for R_w directly. However, by assuming values for R_w, one can determine the value of R_d and a plot of R_d versus R_w can be constructed. The plot will indicate that for a range, R_w, in rain or fog with a radar on a given target, the radar must be capable of detecting that same target at a range R_d in dry air.

Equation 8 is plotted in Figures III-14 through III-22. Figures III-14, 15, 16 and 17

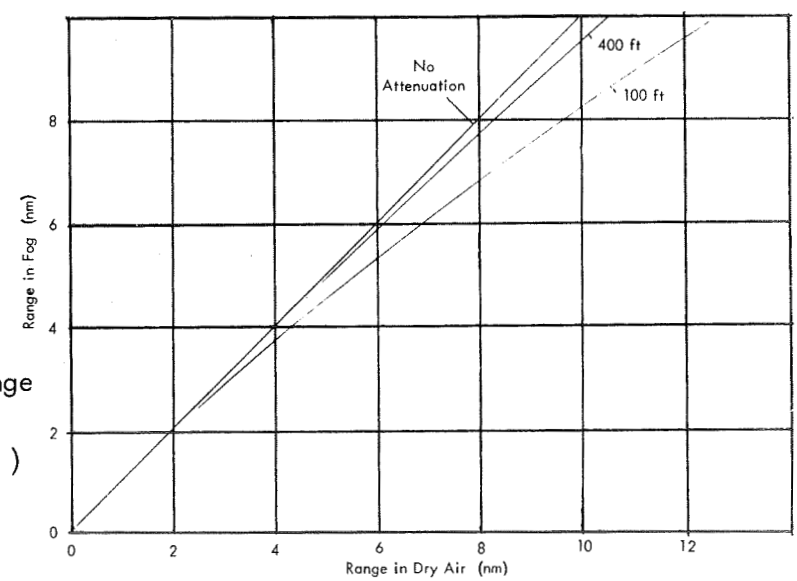

Figure III-14. Reduction in Range for Fog. (X-Band at 18°C)

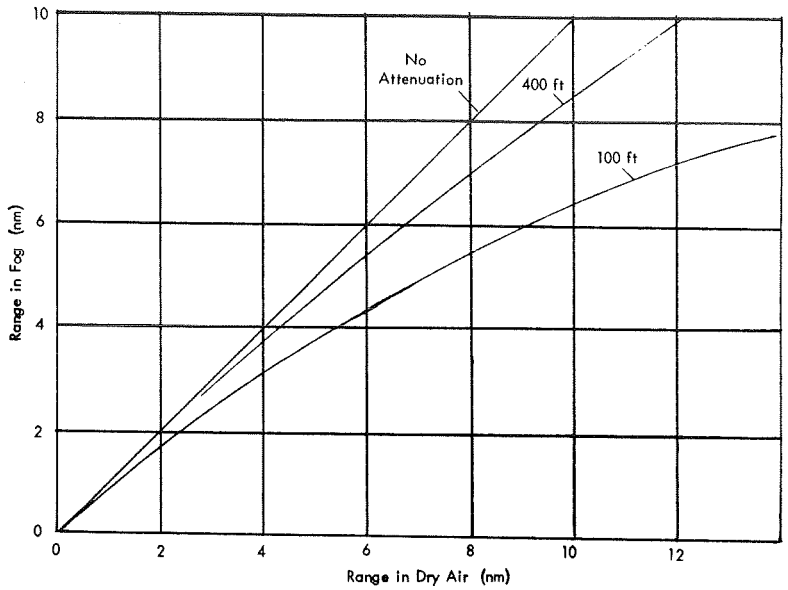

Figure III-15.

Reduction in Range for Fog

(Ku-Band at 18°C)

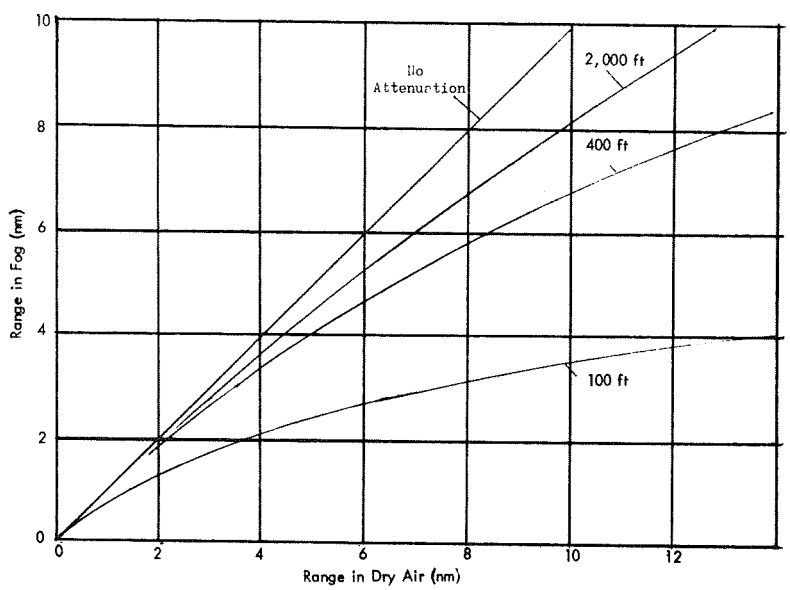

Figure III-16.

Reduction in Range for Fog.

(Ka-Band at 18°C)

indicate the reduction in range from fog at 18°C (γ_a given in Table III-4) and Figures III-19, 20, 21 and 22 indicate the reduction in range from rain attenuation only (γ_a from Table III-5). One should note that since, for a given temperature and meteorological condition, γ_a depends only on frequency, these curves are valid for any pulse radar operating at these frequencies.

In order to predict the range at which a radar can detect a target of given size when the radar signals are attenuated, one must know the range at which that radar can detect that target in dry air. From the radar equation, the power received from a target at Range R with cross section σ is given by:

$$S_r = \frac{PG^2\lambda^2\sigma}{(4\pi)^3 R^4} \qquad (9)$$

where S_r = power received

P = peak power transmitted

G = antenna gain

λ = wave length of radar energy

σ = target cross section

R = radar range

Since we are only considering the effects of attenuation, it will be assumed that a target can be detected if the power received from that target is 6dB greater than the noise power at the radar receiver.

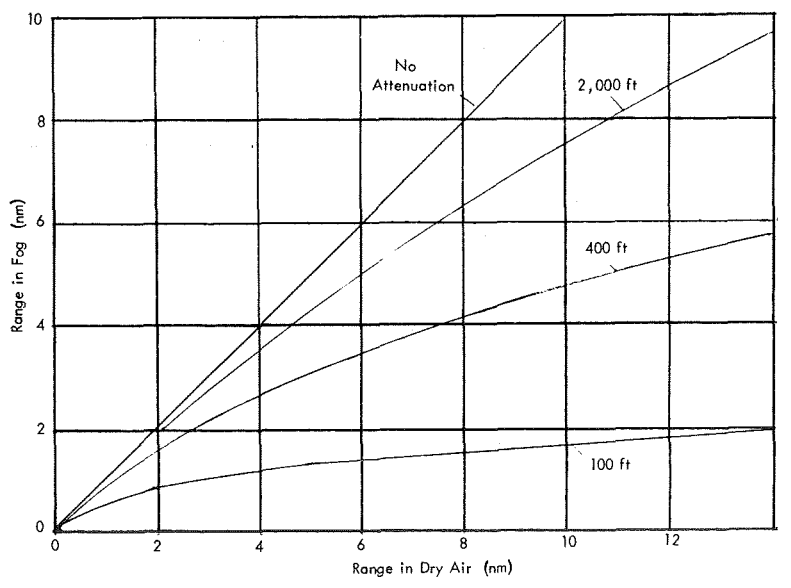

Figure III-17.

Reduction in Range for Fog.

(V-Band at 18°C)

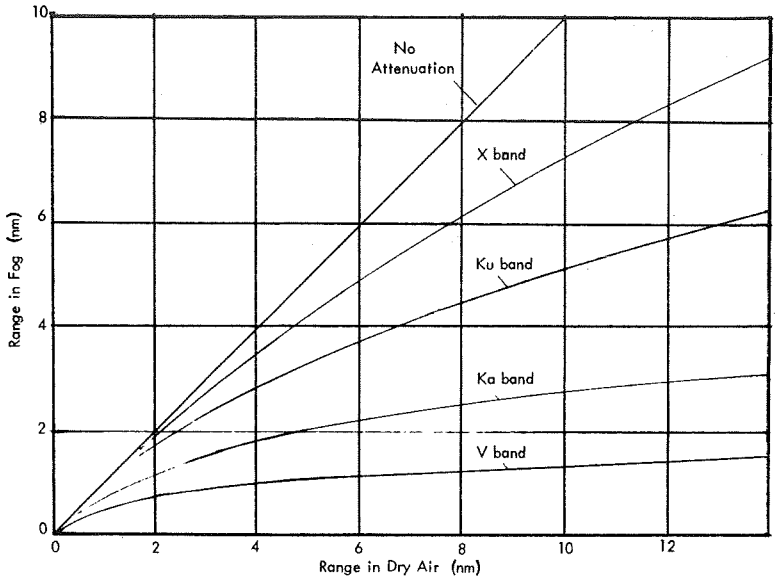

Figure III-18.

Reduction in Range for 100 ft. Visibility Fog at 0°.

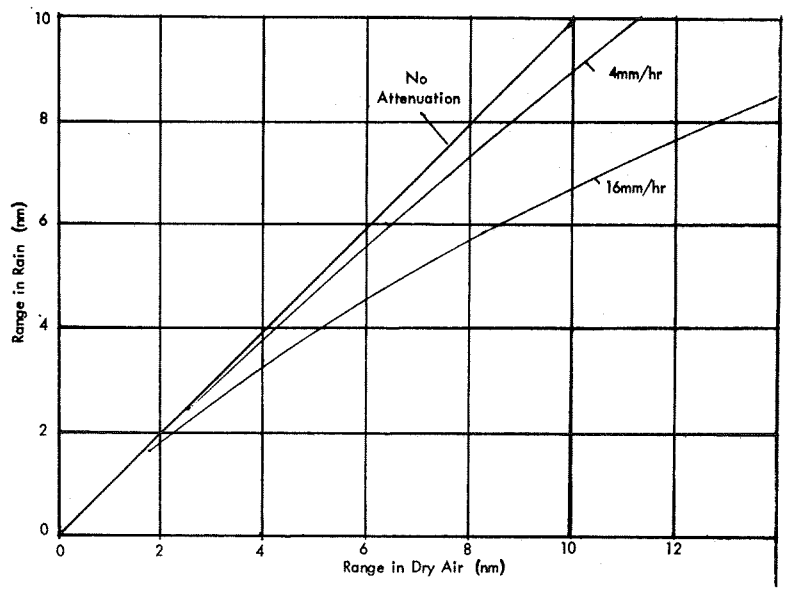

Figure III-19.

Reduction in Range for Rain.

(X-Band at 18°C)

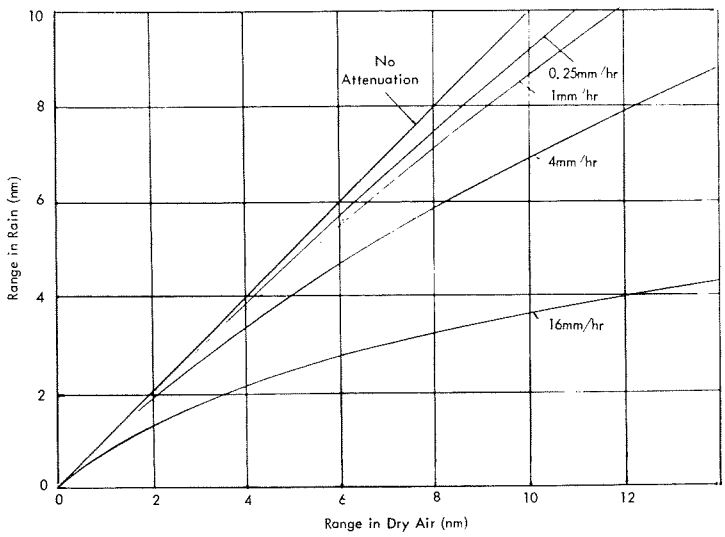

Figure III-20.

Reduction in Range for Rain.

(Ku Band at 18°C)

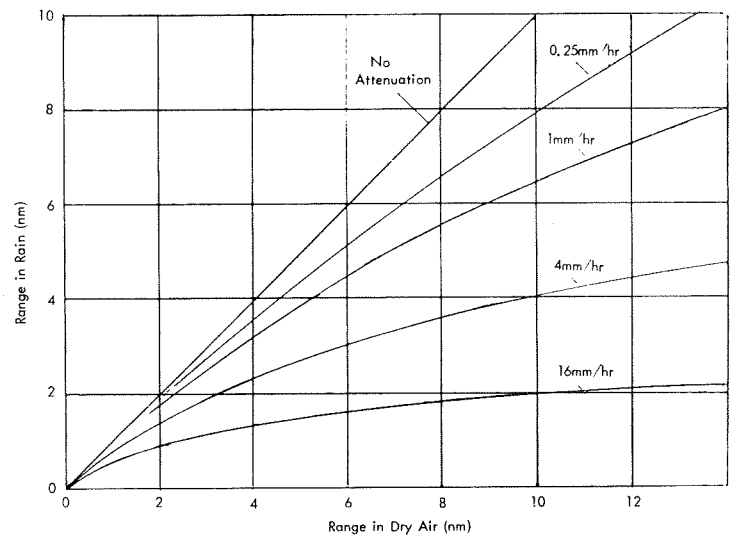

Figure III-21.

Reduction in Range for Rain.

(Ka Band at 18°C)

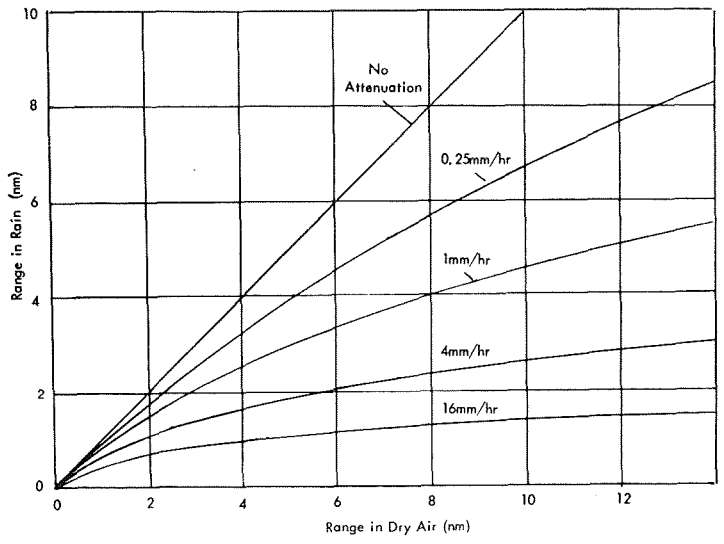

Figure III-22. Reduction in Range for Rain. (V Band at 18°C)

That is: $S_\alpha = P_n + 6dB$

where S_α = power required for reliable detection

P_n = noise power

= kTBN

where k = Boltzmann's constant

T = absolute temperature

B = bandwidth of radar receiver

N = noise figure of radar receiver

To find σ, the radar cross section required for detection at a given range, we rearrange the radar equation to:

$$\sigma = \frac{S_\alpha (4\pi)^3 R^4}{PG^2 \lambda^2} \qquad (10)$$

To proceed further one must assume the parameters of the radar system. Typical parameters for radars which might be used to act as an independent landing monitor are given in Table III-6.

TABLE III-6. TYPICAL PARAMETERS OF RADARS.

Parameters	Frequency Band		
	X	Ku	Ka
Transmitter Peak Power, P	60kW	60kW	60kW
Noise Figure, N	8dB	11dB	14dB
Pulse Length, t	0.05 μs	0.05μs	0.05μs
Bandwidth, B	4×10^7 Hz	4×10^7 Hz	4×10^7 Hz
Wavelength,	3.2 cms	1.8 cms	0.85 cms
Beamwidths	$2.1^\circ \times 8.7^\circ$	$1.2^\circ \times 4.9^\circ$	$0.55^\circ \times 2.3^\circ$
Antenna Gain, G	33dB	38dB	46dB
Receiver Noise, Pn	-120 dBW	-117 dBW	-114 dBW

The ranges in dry air, as a function of target cross section, for the radar parameters assumed above are given in Figure III-23.

To illustrate how one would determine the range in weather, let us suppose $\sigma = 3\ m^2$. Then, the range in dry air for this target is (from Figure III-23):

X band 9.4 nm

Ku band 11 nm

Ka band 15 nm

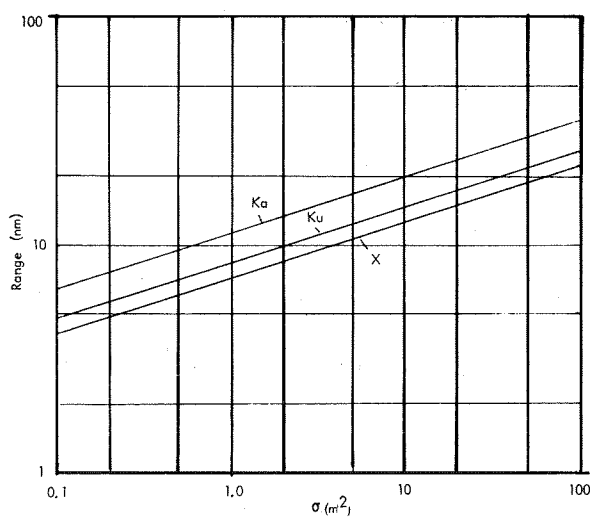

Figure III-23. Unattenuated Radar Range vs Radar Target Cross Section. (Radar Parameters given in Table III-6)

Suppose there is a heavy rain of 16mm/hr. Then, the attenuated range for this $3m^2$ target would be:

X band (from Figure III-19)	6.5nm
Ku band (from Figure III-20)	3.8nm
Ka band (from Figure III-21)	2.2nm

This illustrates how seriously the performance of the higher frequency radars are affected by a heavy rain.

3.5 Degradation of Radar Performance for Extended Targets

Suppose one is interested in detecting an extended target, such as the grass alongside a runway, when the radar signals are attenuated by fog. The extended nature of the target requires that a modification be made to the technique for calculating radar performance when the signals are attenuated. The technique used above can be modified to cover the case where the target fills the radar beam, but a more convenient procedure is given below.

At shallow grazing angles the signal received from the terrain at range R is given by

$$S_t = \frac{PG^2\lambda^2}{(4\pi)^3R^3}\gamma_1\beta\frac{ct}{2}\tan\theta \quad \text{Exp}\ (-2K\gamma_a R) \qquad (11)$$

where P, G, λ, R have conventional meaning

c = propagation velocity

t = transmitted pulse length

θ = grazing angle

β = azimuth beamwidth

γ_1 = scattering coefficient of the terrain

γ_a = attenuation constant due to rain or fog, and

$2K$ = 0.461

The following assumptions are made;

Received signal is 6dB above receiver noise

γ_1 = -15dB at X band

γ_1 = -12dB at Ku band

γ_1 = -12dB at Ka band, and

θ = 3°

With the above assumptions, and with 100 ft visibility fog, Figure III-24 plots S_t versus R for the radars having the parameters given in Table III-6. The threshold levels in this figure represent Receiver noise + 6 dB for each of the three frequencies. The intersection of the signal curve and the threshold curve thus represent the maximum range. The curves show that the maximum ranges are as follows:

X band	18.5km	(10nm)
Ku band	14.5km	(7.8nm)
Ka band	7.5km	(4.1nm)

Bear in mind that the curve of Figures III-23 and III-24 are valid only for the parameters indicated. The curves are not as general as those of the previous figures.

3.6 Conclusions

Figures III-14 through III-22 have some implication on the optimum frequency to use for an IALM radar and/or terrain avoidance radar. Although these curves are directly valid only for small targets they also have implications for detecting extended targets such as terrain or runways. The point to remember is that once the attenuation becomes significant and the curves bend over, there is very little that can be gained by increasing the transmitted power or target cross section. Figures III-14 and III-15 indicate that X band or Ku band radars are capable of achieving ranges of up to 10 nautical miles in a heavy fog although passive augmentation may be required. Figure III-16 indicates a Ka band system can achieve ranges of about 4 1/2 to 5nm in this fog (although once again passive augmentation may be required). These conclusions are substantiated by Figure III-24 for terrain with a fairly high back scattering coefficient. Figure III-17 indicates that a V band set probably cannot achieve a range much greater than 2nm in 100 ft fog, even with passive augmentation.

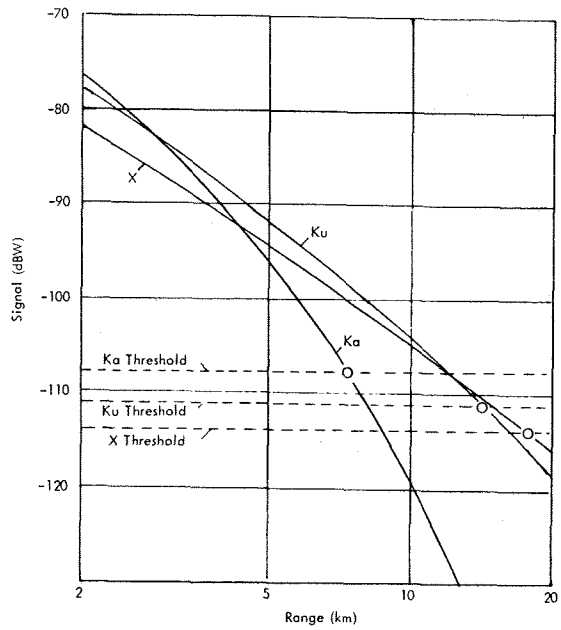

Figure III-24. Range in 100 ft Fog on Grass

When rain is present, the situation becomes more serious. At X band (Figure III-19) a range of 10nm is possible and at Ku band (Figure III-20) a range of 5 to 6nm is possible, again both of these systems might require passive augmentation. However, Figure III-21 indicates that at Ka band the range will not be much more than about 2nm and from Figure III-23, one sees that a V band system will not achieve a range of much more than 1 1/2nm, no matter how large the target.

It should be remembered that the latter set of curves (Figures III-19 through III-22) do not take account of the deleterious effects of the back scatter from rain. Thus, the curves are optimistic for performance in rain and the real situation will be worse than indicated by these curves. These curves indicate that a V band system will probably not have adequate range in fog to serve as an IALM. A Ka band system will probably have adequate performance as an IALM in fog, however, if the system is to operate in heavy rain, frequencies above Ku band will not be suitable. Thus, terrain avoidance or terrain warning systems should operate at Ku or X band.

4.0 BACK SCATTER FROM RAIN

This section defines theoretical values for the radar cross section of rain. The values are used in the calculations of Section 6. The signal received from the rain is given by the equation:

$$S_r = \frac{PG^2\lambda^2\sigma_e}{(4\pi)^3 R^4} \quad \text{Exp}\ (-2K\gamma_a R) \qquad (12)$$

where σ_e = effective radar cross section of rain

P = transmitter peak power

λ = wavelength

$2K$ = a constant

γ_a = attenuation constant

R = range

$\sigma_e = \sigma_u V$

where V = volume in one half pulse length

σ_u = radar cross section of rain per unit volume

$$V = R\alpha R\beta\frac{ct}{2}$$

where α = elevation beamwidth

β = azimuth beamwidth and

beamwidths are given between 3dB points.

The theoretical values of σ_u are shown for four rainfall rates in Figure III-25. These curves have been published by Gunn and East (Ref. 8). The value of σ_u given by their curves for two rainfall rates and three frequencies are listed in Table III-7.

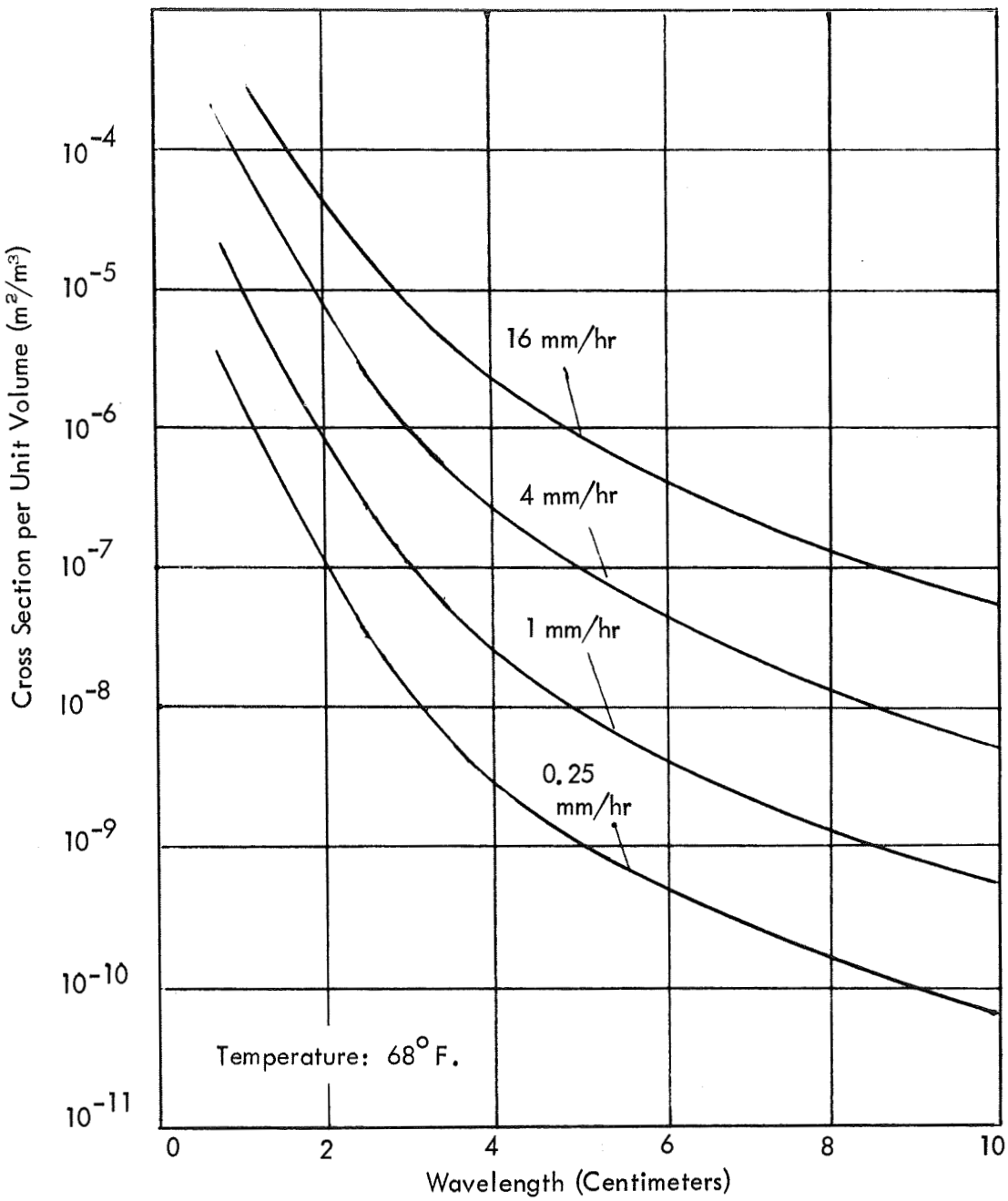

Figure III-25. Theoretical Cross Section per Unit Volume for Various Rainfall Rates

TABLE III-7. THEORETICAL VALUES OF RADAR CROSS SECTION OF RAIN (m^2/m^3)

Rainfall Rate	Frequency Band		
	X	Ku	Ka
4 mm/hr	7×10^{-7}	1.8×10^{-5}	1.6×10^{-4}
16 mm/hr	6.3×10^{-6}	8×10^{-5}	6.5×10^{-4}

It has been found in practice that, due to multiple scattering, the measured values are lower than these theoretical values. But accepted measured values for various rainfall densities, at different frequency bands, are not available and, therefore, in this report the theoretical values are used.

These values of σ_u are for linearly polarized transmission. With circular polarization, the cross section is lower. The amount by which it is lower depends upon how near spherical the rain drops are and, in practice, a typical figure is 15dB, provided the ratio between the two orthogonal components of the signal lies in the interval between 0.82 and 1.22 (cf Panasiewicz, Ref. 9). There is some question whether 15dB cancellation is achieved when a radar is looking at targets with a very low grazing angle (cf McFee, Ref. 10). However, for the calculations in this report, the cross sections listed in Table III-7 will be used and a 15dB cancellation ratio assumed for circular polarization.

5.0 VISIBILITY OF RUNWAYS WITH A MAPPING RADAR

5.1 Introduction

It is well known that an airport runway can be seen on the PPI of an airborne radar. This occurs because the scattering coefficient of the runway is lower than that of the surrounding grass-land. However, it is only seen when the angular resolution of the radar is high enough to pick out the relatively narrow runway. The maximum range at which it is detected depends upon the azimuth beamwidth of the radar's antenna.

No reports have been found with results enabling a reliable prediction to be made of the ability of a given radar to detect runways. In this Section a theoretical estimate is made of the detection range with a given azimuth beamwidth.

5.2 Calculations

The ability to detect a runway depends upon the amount by which the received signal level falls as the radar antenna beam sweeps through the runway. Referring to Figure III-26, the position of the intercept of the beam is shown outside the runway (a), partially covering the runway (b), and in the position for minimum signal (c). The amplitude of the signal received at a given range is the sum of that from grass and from the runway, suitably weighted to take account of the polar diagram and of the different scattering coefficients. For example, in position (a) the amplitude of the received signal is proportional (to a very good approximation) to:

$$2\gamma_1 \int_0^{\infty} \mathrm{Exp}\,(-2K_1 x^2)\,dx \qquad (13)$$

and in position (c) it is proportional to:

$$2\,\gamma_2 \int_0^{\frac{W}{2}} \mathrm{Exp}\,(-2K_1 x^2)\,dx + 2\,\gamma_1 \int_{\frac{W}{2}}^{\infty} \mathrm{Exp}\,(-2K_1 x^2)\,dx \qquad (14)$$

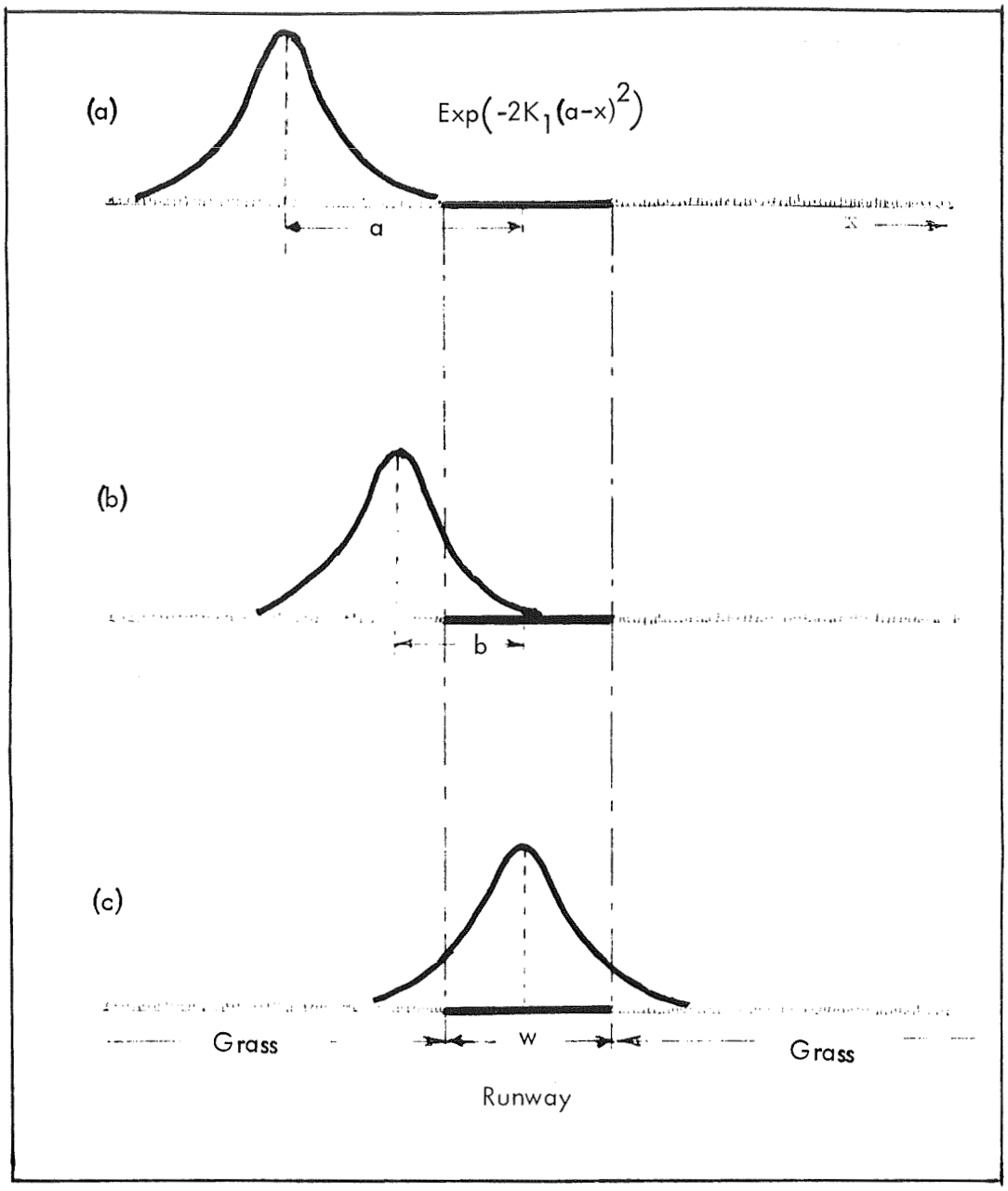

Figure III-26. Beam Intercept on Runway

where w = runway width

$\text{Exp}\ (-2K_1 x^2)$ = polar diagram weighting factor

K_1 = a constant which depends upon beamwidth and range

$= \dfrac{2.572}{R^2\ \beta^2}$

R = range to runway

β = beamwidth between 3dB points in radians

γ_1 = scattering coefficient of grass

γ_2 = scattering coefficient of runway surface

The ability of the radar to detect a runway depends upon the ratio:

$$\frac{2\,\gamma_1 \int_0^{\infty} \text{Exp}\ (-2K_1 x^2)\, dx}{2\,\gamma_2 \int_0^{\frac{w}{2}} \text{Exp}\ (-2K_1 x^2)\, dx + 2\,\gamma_1 \int_{\frac{w}{2}}^{\infty} \text{Exp}\ (-2K_1 x^2)\, dx} \qquad (15)$$

By substituting y^2 for $2K_1 x^2$, the ratio becomes:

$$\frac{\gamma_1 \int_0^{\infty} \text{Exp}\ (-y^2)\ dy}{\gamma_2 \int_0^{\frac{w}{2}(2K_1)^{1/2}} \text{Exp}\ (-y^2)\, dy + \gamma_1 \int_{\frac{w}{2}(2K_1)^{1/2}}^{\infty} \text{Exp}\ (-y^2)\, dy}$$

$$= \frac{1}{\frac{\gamma_2}{\gamma_1} \operatorname{Erf}\left(\frac{w}{2}(2K_1)^{1/2}\right) + 1 - \operatorname{Erf}\left(\frac{w}{2}(2K_1)^{1/2}\right)}$$

where $\operatorname{Erf}(y) = \frac{2}{\sqrt{\pi}} \int_0^y \operatorname{Exp}(-y^2)\, dy$

$$= \frac{1}{1 - \operatorname{Erf}\left(\frac{w}{2}(2K_1)^{1/2}\right)\left(1 - \frac{\gamma_2}{\gamma_1}\right)} \qquad (16)$$

Assuming that a fall in the received signal level of 3dB, as the antenna beam passes through the runway, is the minimum requirement for visibility on a display, the criterion for runway detection is given by the equation:

$$\operatorname{Erf}\left(\frac{w}{2}(2K_1)^{1/2}\right)\left(1 - \frac{\gamma_2}{\gamma_1}\right) = 0.5 \qquad (17)$$

Substitution for K gives:

$$\operatorname{Erf}\left(\frac{1.14w}{R\beta}\right)\left(1 - \frac{\gamma_2}{\gamma_1}\right) = 0.5$$

or, when β is expressed in degrees,

$$\operatorname{Erf}\left(\frac{65w}{R\beta}\right)\left(1 - \frac{\gamma_2}{\gamma_1}\right) = 0.5 \qquad (18)$$

By substitution in Equation 18 the following table is obtained giving the runway detection range, R, in nautical miles, at which a 3dB fall in signal occurs as the beam sweeps through the runway, for various azimuth beamwidths and scattering coefficient ratios.

TABLE III-8. RUNWAY DETECTION RANGE (nm)

$\frac{\gamma_1}{\gamma_2}$	300 ft wide Runway				150 ft wide Runway			
	Azimuth Beamwidth				Azimuth Beamwidth			
dB	2.5°	1.5°	0.7°	0.35°	2.5°	1.5°	0.7°	0.35°
4	1.33	2.2	4.73	9.45	0.67	1.1	2.37	4.73
6	1.86	3.1	6.68	13.4	0.93	1.55	3.34	6.7
10	2.36	3.94	8.5	17.0	1.18	1.97	4.25	8.5
13	2.5	4.20	9.0	18.0	1.25	2.10	4.5	9.0
16	2.61	4.36	9.3	18.6	1.31	2.18	4.65	9.3
20	2.68	4.44	9.6	19.2	1.34	2.22	4.8	9.6

These results are plotted on Figure III-27. It is interesting to note that increasing the Grass/Runway scattering coefficient above 10dB makes little difference to the detection range.

When γ_1 / γ_2 = 10dB, the fall in signal is given by the expression:

$$10 \log \frac{1}{1-0.9 \text{ Erf } \left(\frac{65w}{R\beta}\right)} \qquad (19)$$

The fall for various ranges and beamwidths is listed below, for a runway width of 300 ft.

TABLE III-9. SIGNAL FALL (dB) FOR 300 FT RUNWAY.
(Grass/Runway Scattering Coefficient Ratio = 10 dB)

Range (nm)	Azimuth Beamwidth			
	2.5°	1.5°	0.7°	0.35°
1	7.8	9.9	10	10
2	3.8	6.7	9.9	10
3	2.2	4.2	8.9	10
4	1.7	3.0	7.2	9.9
5	1.3	2.2	5.6	9.5
10	0.65	1.0	2.5	5.6

These results, showing the rapid increase in signal fall as the range decreases, are plotted in Figure III-28.

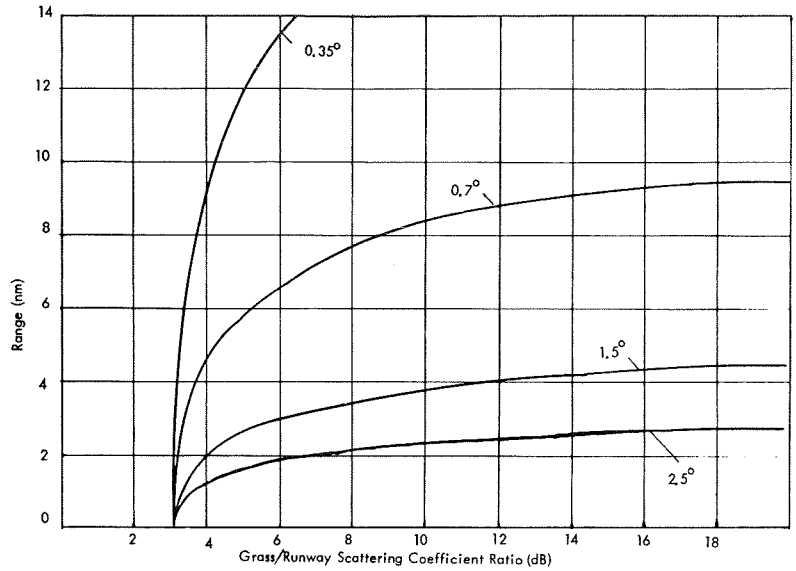

Figure III-27. Detection Range of 300 ft Runway for Various Azimuth Beamwidths

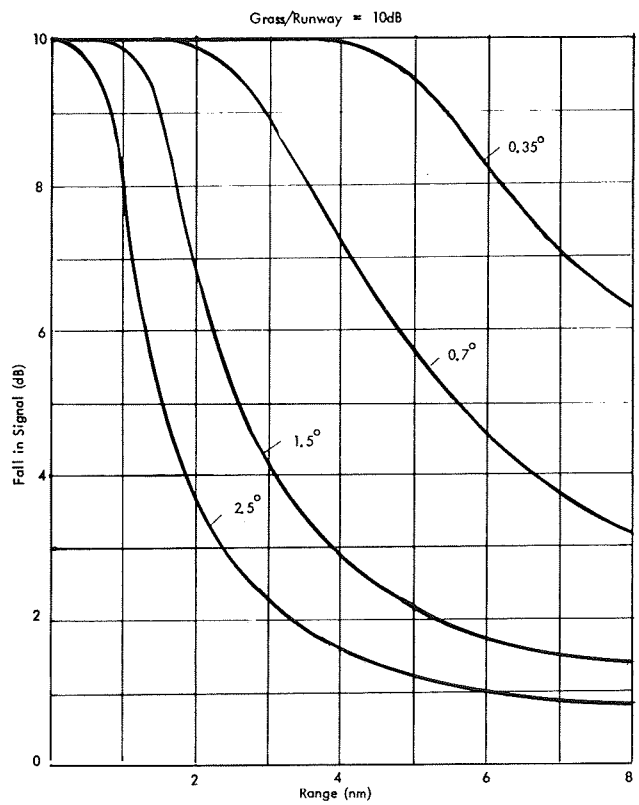

Figure III-28. Fall in Signal as Beam Sweeps Through 300 ft Runway

When the grass/runway scattering coefficient ratio is 20dB, the following table gives the signal fall as the beam sweeps through a 300 ft wide runway for various ranges. These figures are plotted in Figure III-29.

TABLE III-10. SIGNAL FALL (dB) FOR 300 FT RUNWAY.
(Grass/Runway Scattering Coefficient Ratio = 20 dB)

Range (nm)	Azimuth Beamwidth			
	2.5°	1.5°	0.7°	0.35°
1	11	19.2	20	20
2	4.4	8.7	19.2	20
3	2.7	5.0	14	20
4	1.8	3.5	9.4	19.2
5	1.4	2.5	7.0	17
10	1.07	1.13	2.88	7.0

Figure III-29. Fall in Signal as Beam Sweeps Through 300 ft Runway

Grass/Runway Scattering Coefficient = 20 dB

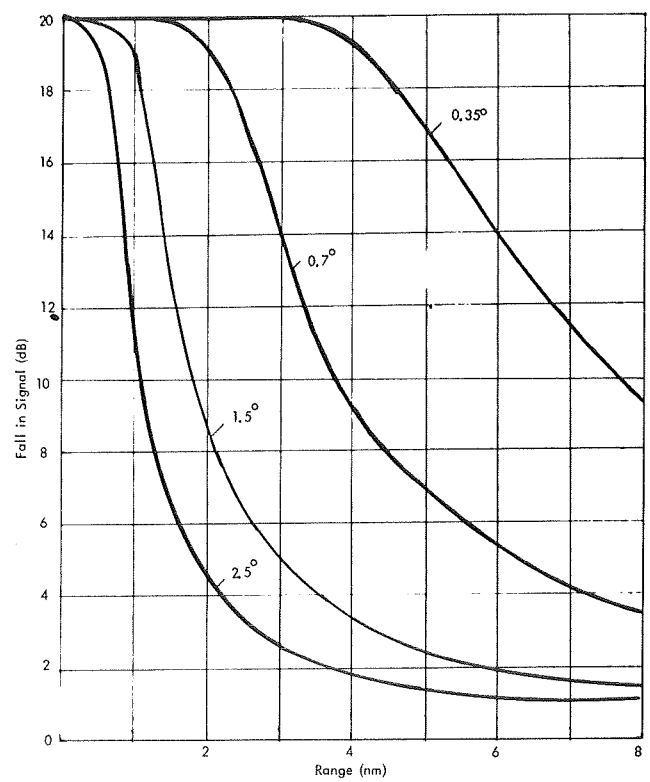

Figure III-29. Fall in Signal as Beam Sweeps Through 300 ft. Runway.

6.0 SIGNAL LEVEL CALCULATIONS

This section contains the calculations of signal levels and signal level ratios which are used to characterize the radar sensor.

6.1 Signal Reflected from Grassy Terrain

The signal reflected from the terrain is given by equation 7 as:

$$S_t = \frac{PG^2\lambda^2}{(4\pi)^3 R^3} \gamma\beta \frac{tc}{2} \tan\theta \, \psi^2 \text{ watts} \qquad (20)$$

where
- P = Transmitter peak power (watts)
- G = Antenna gain
- t = Pulse length (seconds)
- c = Velocity of propogation (meters/second)
- θ = Grazing angle (degrees)
- γ = Scattering coefficient
- β = Aximuth beamwidth (radians)
- λ = Wave length (meters)
- ψ = One-way attenuation term, Exp $(-K\gamma_a R)$
- R = Range (meters)

For all the frequency bands θ is taken at 3° and the scattering coefficient, γ, for grass is assumed to be -13dB. Expressed in dB, the parameters for the radars listed in Volume II (this report) are given in the following table.

TABLE III-11. RADAR PARAMETERS (dB)

Parameters	Frequency Band			
	X	Ku	Ka	V
[P]	43	43	43	40
[G]	33.2	37.7	41.6	44.6
[α]	-8.8	-10.7	-11.5	-11.5
[β]	-13.6	-15.7	-19	-22
[λ^2]	-30.5	-34.4	-41.4	-47.3
[N]	10	12	16	25

Inserting the above values in Equation 20 , the following equations for the various frequency bands are obtained:

X band $[S_t] = 88.3 + [t] + 2[\psi] - 3[R]$ dBW (21)

Ku band $[S_t] = 91.3 + [t] + 2[\psi] - 3[R]$ dBW (22)

Ka band $[S_t] = 88.8 + [t] + 2[\psi] - 3[R]$ dBW (23)

V band $[S_t] = 82.9 + [t] + 2[\psi] - 3[R]$ dBW (24)

6.2 Receiver Noise

The receiver noise is given by the equation,

$$N_r = \frac{400BN}{10^{23}} \tag{25}$$

where B = Receiver bandwidth

N = Receiver Noise Figure

Assuming the receiver bandwidth is the typical value, 1/t Hz, Equation 25, expressed in dB, becomes:

$$[N_r] = -204 + [N] - [t] \tag{26}$$

Inserting the values for N, given in Table III-11 gives:

X band	$[N_r] = -194 - [t]$		(27)
Ku band	$[N_r] = -192 - [t]$		(28)
Ka band	$[N_r] = -188 - [t]$		(29)
V band	$[N_r] = -179 - [t]$		(30)

6.3 Signal Reflected from Rain

The amplitude of the signal reflected from rain is given by the equation:

$$S_r = \frac{PG^2\lambda^2}{(4\pi)^3 R^2} \sigma_u \alpha\beta \frac{tc}{2} \psi^2 \text{ watts} \tag{31}$$

where α = Elevation antenna beamwidth (radians)

σ_u = Scattering cross section of rain (meter^2/meter^3)

With the values given in Table III-11, the following equations for the various bands are derived:

X band	$[S_r] = 105.3 + [t] + [\sigma_u] - 2[R] + 2[\psi]$ dBW		(32)
Ku band	$[S_r] = 106.4 + [t] + [\sigma_u] - 2[R] + 2[\psi]$ dBW		(33)
Ka band	$[S_r] = 103.1 + [t] + [\sigma_u] - 2[R] + 2[\psi]$ dBW		(34)
V band	$[S_r] = 97.2 + [t] + [\sigma_u] - 2[R] + 2[\psi]$ dBW		(35)

6.4 Signal Reflected from a Reflector

The signal reflected from a corner reflector with an echoing area of σ meter^2 is given by the equation:

$$S_c = \frac{PG^2\lambda^2\sigma}{(4\pi)^3 R^4} \psi^2 \text{ watts} \tag{36}$$

With the parameters listed in Table III-11, the following equations are obtained:

X band $[S_c] = 45.9 + [\sigma] - 4[R] + 2[\psi]$ dBW (37)

Ku band $[S_c] = 51.0 + [\sigma] - 4[R] + 2[\psi]$ dBW (38)

Ka band $[S_c] = 51.8 + [\sigma] - 4[R] + 2[\psi]$ dBW (39)

V band $[S_c] = 48.9 + [\sigma] - 4[R] + 2[\psi]$ dBW (40)

6.5 Ratio of Terrain Signal to Receiver Noise

From equations 21 through 24 and 27 through 30 the following is obtained:

X band $[S_t/N_r] = 282.3 + 2[t] - 3[R] + 2[\psi]$ (41)

Ku band $[S_t/N_r] = 283.3 + 2[t] - 3[R] + 2[\psi]$ (42)

Ka band $[S_t/N_r] = 276.8 + 2[t] - 3[R] + 2[\psi]$ (43)

V band $[S_t/N_r] = 261.9 + 2[t] - 3[R] + 2[\psi]$ (44)

By substitution, the following equations are obtained for the conditions that make $[S_t/N_r] = 10$.

X band $3[R] - 2[\psi] = 272.3 + 2[t]$ (45)

Ku band $3[R] - 2[\psi] = 273.3 + 2[t]$ (46)

Ka band $3[R] - 2[\psi] = 266.8 + 2[t]$ (47)

V band $3[R] - 2[\psi] = 251.9 + 2[t]$ (48)

Table III-12 lists values of $2[\psi]$ obtained from the attenuation values given in Section 3, Volume III.

Values of $3[R] - 2[\psi]$ are plotted in Figures III-30 through III-33 against R for various weather conditions and from these curves the values listed in Table III-13 have been obtained for the range at which $S_t/N_r = 10$.

TABLE III-12. VALUES OF $-2[\psi]$ (dB)

Frequency Band	R km	[R] dB	Rainfall Rates 1mm/hr	4mm/hr	16mm/hr	Fog Densities 400 ft	100 ft
X	1	30	0.02	0.10	0.52	0.04	0.20
	2	33	0.04	0.20	1.04	0.08	0.40
	4	36	0.08	0.40	2.08	0.16	0.80
	10	40	0.20	1.0	5.2	0.40	2.0
	20	43	0.40	2.0	10.4	0.80	4.0
	40	46	0.80	4.0	20.8	1.6	8.0
	100	50	2.0	10.0	52	4.0	20.0
Ku	1	30	0.14	0.50	2.56	0.16	0.72
	2	33	0.28	1.0	5.12	0.32	1.44
	4	36	0.56	2.0	10.24	0.64	2.88
	10	40	1.4	5.0	25.6	1.6	7.2
	20	43	2.8	10	51.2	3.2	14.4
	40	46	5.6	20	102.4	6.4	28.8
	100	50	14	50	256	16	72
Ka	1	30	0.6	2.14	8.14	0.54	2.78
	2	33	1.2	4.28	16.28	1.08	5.56
	4	36	2.4	8.56	32.56	2.16	11.12
	10	40	6.0	21.4	81.4	5.4	27.8
	20	43	12	42.8	162.8	10.8	55.6
	40	46	24	85.6	325.6	21.6	111.2
	100	50	60	214	814	54	278
V	1	30	1.6	4.80	14.6	1.44	10.24
	2	33	3.2	9.6	29.2	2.88	20.48
	4	36	6.4	19.2	58.4	5.76	40.96
	10	40	16	48	146	14.4	102.4
	20	43	32	96	292	28.8	204.8
	40	46	64	192	584	57.6	409.6
	100	50	160	480	1460	144	1024

TABLE III-13. RANGE (km) AT WHICH TERRAIN SIGNAL / NOISE = 10dB

Frequency band	Pulse Length	Rainfall Rates				Fog Densities	
	μs	0 mm/hr	1 mm/hr	4 mm/hr	16 mm/hr	400 ft	100 ft
X	1.0	118	100	69	32	88	53
	0.5	76	66	50	25	60	40
	0.1	26	25	22	14	24	20
Ku	1.0	130	68	35	12	60	28
	0.5	82	50	28	11	45	22
	0.1	28	23	15	7	21	13
Ka	1.0	80	23	12	4.5	26	9.5
	0.5	47	20	9.6	4	20	8
	0.1	17	10	6	2.7	11	5
V	1.0	26	8.3	4.7	2.2	9.2	2.8
	0.5	16	6.6	3.9	1.9	7.4	2.4
	0.1	5.5	3.5	2.4	1.3	4.0	1.6

Table III-14 lists the ranges at which S_t/N_r = 20dB for various weather conditions and transmitter pulse lengths.

TABLE III-14 RANGE (km) AT WHICH TERRAIN SIGNAL / NOISE = 20dB

Frequency Band	Pulse Length μs	Rainfall Rates				Fog Densities	
		0 mm/hr	1 mm/hr	4 mm/hr	16 mm/hr	400 ft	100 ft
X	1.0	55	52	41	22	48	33
	0.5	35	33	28	16	31	24
	0.1	12	12	11	8.0	11	10
Ku	1.0	60	41	24	9.5	38	20
	0.5	35	27	17	7.2	25	14
	0.1	12	11	8.4	4.5	10	7.1
Ka	1.0	36	18	8.8	3.5	16	7.4
	0.5	23	13	7.1	3.1	12	6.0
	0.1	7.9	6.0	4.1	2.1	5.8	3.6
V	1.0	11	5.5	3.4	1.7	6.0	2.1
	0.5	7.3	4.3	2.8	1.4	4.7	1.8
	0.1	2.5	2.0	1.5	0.8	2.2	1.0

6.6 Ratio of Terrain Signal to Rain Signal

From Equations 21 through 24 and 32 through 35 the following equations are obtained for S_t/S_r:

X band $[S_t/S_r] = -17.0 - [\sigma_u] - [R]$ (49)

Ku band $[S_t/S_r] = -15.1 - [\sigma_u] - [R]$ (50)

Ka band $[S_t/S_r] = -14.3 - [\sigma_u] - [R]$ (51)

V band $[S_t/S_r] = -14.3 - [\sigma_u] - [R]$ (52)

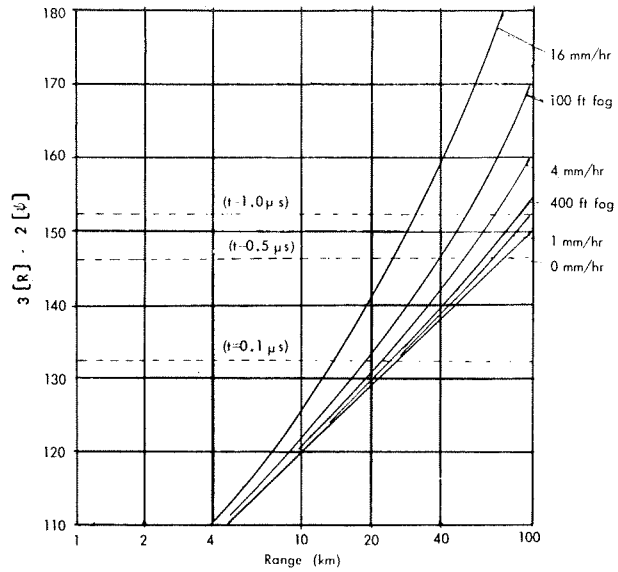

Figure III-30. Values of 3 [R] - 2 [ψ] for X band.

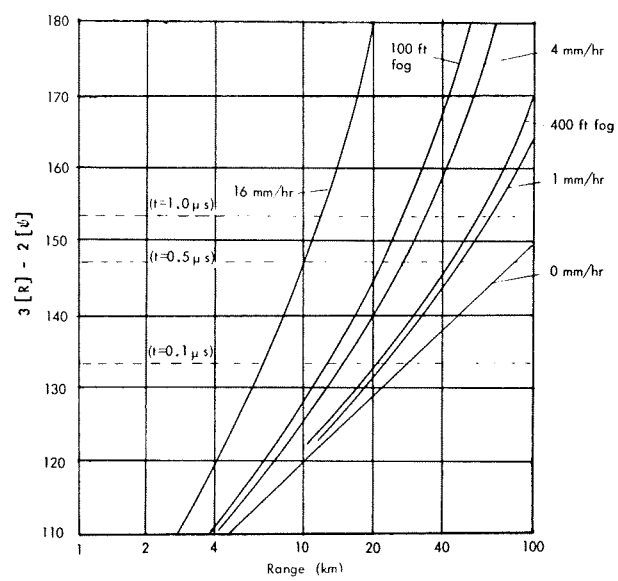

Figure III-31. Values of 3 [R] - 2 [ψ] for Ku band.

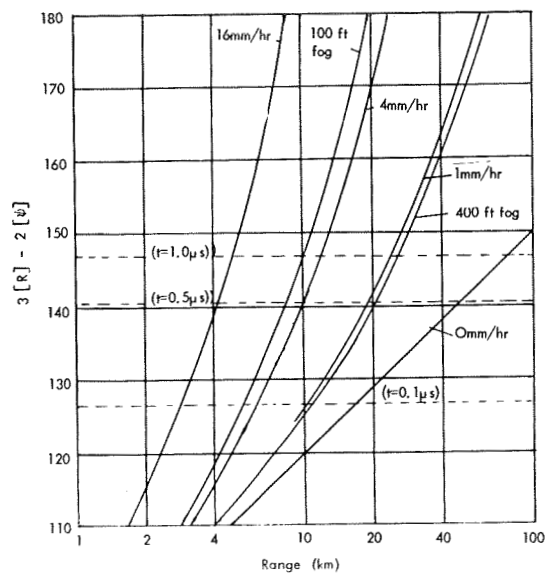

Figure III-32. Values of 3 [R] - 2 [ψ] for Ka band.

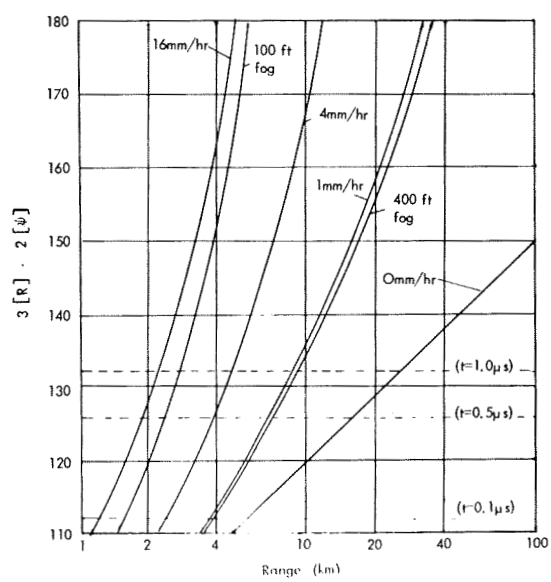

Figure III-33. Values of 3 [R] - 2 [ψ] for V band.

The conditions for $[S_t/S_r] = 10$ are:

X band $[R] = -27 - [\sigma_u]$ (53)

Ku band $[R] = -25.1 - [\sigma_u]$ (54)

Ka band $[R] = -24.3 - [\sigma_u]$ (55)

V band $[R] = -24.3 - [\sigma_u]$ (56)

Taking the values of the scattering cross section of rain, σ_u, from Section 4, the following values (Table III-15) are obtained for R, when $[S_t/S_r] = 10$. The values of $[\sigma_u]$ listed for Ku, Ka and V bands include the 15 dB reduction due to cancellation which occurs with circular polarization.

TABLE III-15. RANGE (km) FOR TERRAIN SIGNAL/RAIN SIGNAL = 10.

Frequency Band	Parameter Band	Rainfall Rates		
		1 mm/hr	4 mm/hr	16 mm/hr
X (linear polarization)	$[\sigma_u]$	-69	-60	-50
	[R]	42	33	23
	R (km)	16	2.0	0.2
Ku (Circular Polarization)	$[\sigma_u]$	-74	-65	-57
	[R]	48.9	39.9	31.9
	R (km)	77	9.8	1.5
Ka (Circular Polarization)	$[\sigma_u]$	-62	-54	-47
	[R]	37.7	29.7	22.7
	R (km)	5.9	0.93	0.19
V (Circular Polarization)	$[\sigma_u]$	-51	-42	-36
	[R]	26.7	17.7	11.7
	R (km)	0.47	0.059	0.015

6.7 Ratio of Reflector Signal to Receiver Noise

From Equations 37 through 40 and 27 through 30, the following equations are derived:

X band $[S_c/N_r] = 239.9 + [\sigma] + [t] - 4[R] + 2[\psi]$ (57)

Ku band $[S_c/N_r] = 243.0 + [\sigma] + [t] - 4[R] + 2[\psi]$ (58)

Ka band $[S_c/N_r] = 239.8 + [\sigma] + [t] - 4[R] + 2[\psi]$ (59)

V band $[S_c/N_r] = 227.9 + [\sigma] + [t] - 4[R] + 2[\psi]$ (60)

The conditions for $S_c/N_r = 10$ are:

X band $4[R] - 2[\psi] = 229.9 + [\sigma] + [t]$ (61)

Ku band $4[R] - 2[\psi] = 233.0 + [\sigma] + [t]$ (62)

Ka band $4[R] - 2[\psi] = 229.8 + [\sigma] + [t]$ (63)

V band $4[R] - 2[\psi] = 217.9 + [\sigma] + [t]$ (64)

Taking the values of $2[\psi]$ given in Table III-12, Figures III-34 through III-37 are obtained showing the variations of $4[R] - 2[\psi]$ with R. From these curves the values of R that satisfy Equations 61, 62, 63 and 64 with a 1000 meter^2 reflector are obtained and these are listed in Table III-16.

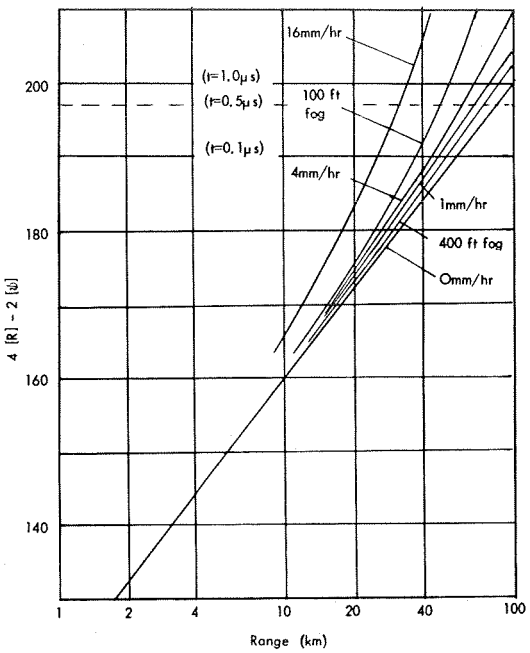

Figure III-34. 4 [R] -2 [ψ] for X band.

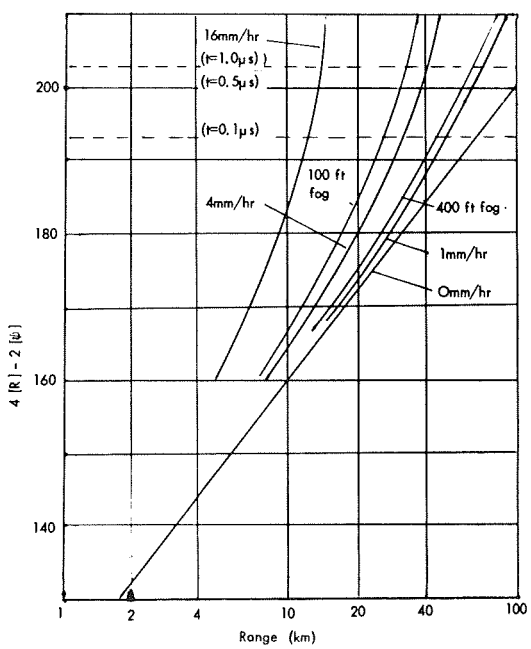

Figure III-35. 4 [R] - 2 [ψ] for Ku band.

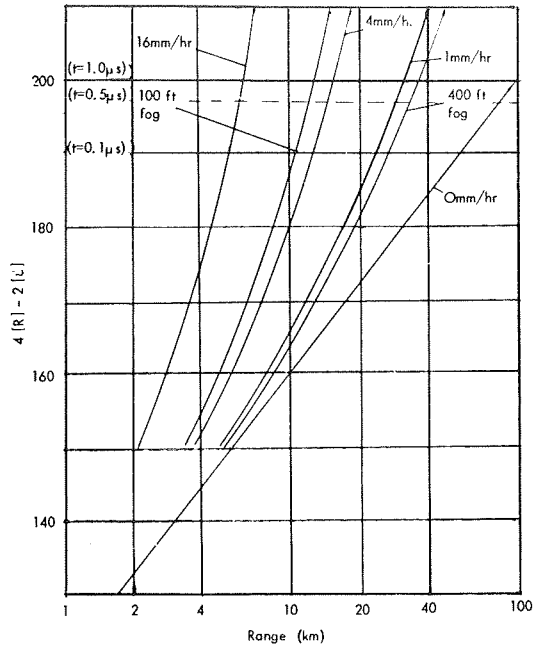

Figure III-36. 4 [R] - 2 [ψ] for Ka band.

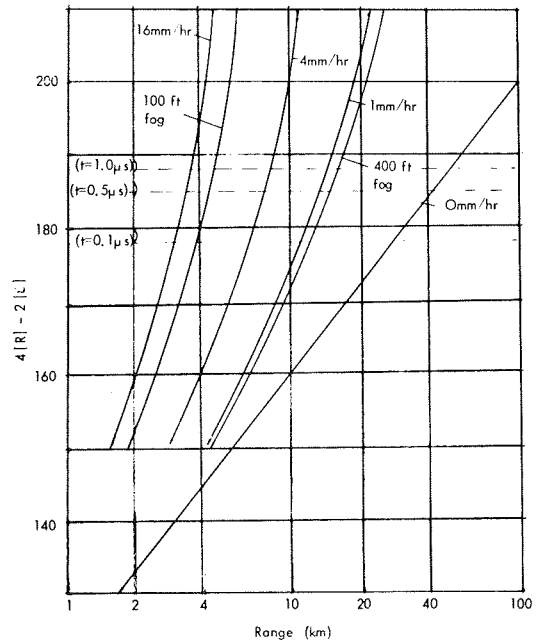

Figure III-37. 4 [R] - 2 [ψ] for V band.

TABLE III-16. RANGE (km) ON $1000m^2$ REFLECTOR, SIGNAL/NOISE = 10.

Frequency Band	Pulse Length	Rainfall Rates				Fog Densities	
	μs	0 mm/hr	1 mm/hr	4 mm/hr	16 mm/hr	100 ft	400 ft
X	1.0	100	90	68	34	82	52
	0.5	84	74	61	32	70	47
	0.1	56	51	44	26	47	36
Ku	1.0	120	70	41	14	63	33
	0.5	100	63	38	13	58	31
	0.1	67	50	31	12	44	26
Ka	1.0	100	32	15	6.0	36	13
	0.5	84	30	14	5.7	32	12
	0.1	56	23	12	5.1	26	10
V	1.0	50	14	7.4	3.4	15	4.3
	0.5	43	13	7.0	3.2	14	4.1
	0.1	28	10	5.9	2.8	11	3.5

6.8 Ratio of Reflector Signal to Terrain Signal

Values for S_c/S_t are obtained from Equations 37 through 40 and 21 through 24 and these are listed below:

X band $[S_c/S_t] = -42.4 + [\sigma] - [t] - [R]$ (65)

Ku band $[S_c/S_t] = -40.3 + [\sigma] - [t] - [R]$ (66)

Ka band $[S_c/S_t] = -37.0 + [\sigma] - [t] - [R]$ (67)

V band $[S_c/S_t] = -34.0 + [\sigma] - [t] - [R]$ (68)

The ranges for S_c/S_t to be equal to 10 when $\sigma = 1000m^2$ are given by the following equations and the results listed in Table III-17 for various pulse lengths.

X band $[R] = -22.4 - [t]$ (69)

Ku band $[R] = -20.3 - [t]$ (70)

Ka band $[R] = -17.0 - [t]$ (71)

V band $[R] = -14.0 - [t]$ (72)

TABLE III-17. RANGE (km) AT WHICH REFLECTOR SIGNAL/TERRAIN SIGNAL = 10.

Frequency Band	Pulse Width		
	t = 1.0 μs	t = 0.5 μs	t = 0.1 μs
X	5.7	11	57
Ku	9.3	19	93
Ka	20	40	200
V	40	80	400

6.9 Ratio of Reflector Signal to Rain Signal ($S_c S_r$)

From Equations 37 through 40 and 32 through 35, the following equations are obtained for S_c/S_r:

X band $[S_c/S_r] = -59.4 + [\sigma] - 2[R] - [t] - [\sigma_u]$ (73)

Ku band $[S_c/S_r] = -55.4 + [\sigma] - 2[R] - [t] - [\sigma_u]$ (74)

Ka band $[S_c/S_r] = -51.3 + [\sigma] - 2[R] - [t] - [\sigma_u]$ (75)

V band $[S_c/S_r] = -48.3 + [\sigma] - 2[R] - [t] - [\sigma_u]$ (76)

When σ is $1000m^2$, the ranges at which $[S_c/S_r] = 10$ are given by the following equations:

X band $2[R] = -39.4 - [t] - [\sigma_u]$ (77)

Ku band $2[R] = -35.4 - [t] - [\sigma_u]$ (78)

Ka band $2[R] = -31.3 - [t] - [\sigma_u]$ (79)

V band $2[R] = -28.3 - [t] - [\sigma_u]$ (80)

The values of R for various values of t and σ_u are listed in the following Table (III-18).

TABLE III-18. RANGE (km) AT WHICH REFLECTOR SIGNAL/RAIN SIGNAL = 10.

Frequency Band	Pulse Length μs	Rainfall 1 mm/hr	4 mm/hr	16 mm/hr
X (Linear Polarization)	1.0	30	11	3.4
	0.5	43	15	4.8
	0.1	95	34	11
Ku (Circular Polarization)	1.0	85	30	12
	0.5	120	42	17
	0.1	265	94	37
Ka (Circular Polarization)	1.0	35	14	6.1
	0.5	49	19	8.6
	0.1	110	43	19
V (Circular Polarization)	1.0	14	4.9	2.5
	0.5	19	6.7	3.4
	0.1	44	15	7.8

6.10 Reflector Size for S_c/S_t = 10dB

By substituting in Equations 65 through 68 the reflector size, to give a reflector signal to terrain signal ratio of 10dB, is given by the following equations:

X band $[\sigma] = 52.4 + [t] + [R]$ (81)

Ku band $[\sigma] = 50.3 + [t] + [R]$ (82)

Ka band $[\sigma] = 47.0 + [t] + [R]$ (83)

V band $[\sigma] = 44.0 + [t] + [R]$ (84)

At a range of 300m the corner reflector size required is listed below.

TABLE III-19. SIZE OF REFLECTOR TO GIVE S_c/S_t OF 10dB AT A RANGE OF 300m.

Frequency Band	Pulse Length, μs	Reflector Area (m^2)
X	1.0	52
	0.5	26
	0.1	5.2
Ku	1.0	32
	0.5	16
	0.1	3.2
Ka	1.0	15
	0.5	7.5
	0.1	1.5
V	1.0	7.5
	0.5	3.8
	0.1	0.75

6.11 Pulse Length and Reflector Size for S_c/N_r and S_c/S_t to be 10 dB at a Given Range in 100 ft Visibility Fog

- X band

The condition for $[S_c/N_r] = 10$ is from Equation 61

$$4[R] - 2[\psi] - 229.9 = [\sigma] + [t] \tag{84}$$

From Equation 65 is obtained when $[S_c/S_t] = 10$

$$[R] + 52.4 = [\sigma] - [t] \tag{85}$$

Solving these two simultaneous equations for various values of R with values of ψ for a 100 ft visibility fog gives the following values for σ and t.

TABLE III-20. OPTIMUM PULSE LENGTH AND MINIMUM REFLECTOR SIZE FOR X BAND IN 100 FT VISIBILITY FOG.

	Range (km)				
	1	2	4	10	20
[R]	30	33	36	40	43
4 [R]	120	132	144	160	172
-2 [ψ]	0.2	0.4	0.8	2.0	4.0
4 [R] - 2 [ψ]	120.2	132.4	144.8	162.0	176.0
4 [R] - 2 [ψ] - 229.9	-109.7	- 97.5	- 85.1	- 67.9	- 53.9
[R] + 52.4	82.4	85.4	88.4	92.4	95.4
2 [σ]	- 27.3	- 12.1	+ 3.3	+ 24.5	+ 41.5
2 [t]	-192.1	-182.9	-173.5	-160.3	-149.3
[σ]	- 13.7	- 6.1	+ 1.7	+ 12.3	+ 20.8
σ (m^2)	0.04	0.2	1.5	17	120
[t]	- 96.1	- 91.5	- 86.8	- 80.2	- 74.7
t (μs)	0.0002	0.0007	0.002	0.01	0.03

In 16mm/hr rain, the optimum reflector size and pulse length for a detection range of 20 km are, from substitution in Equations 84 and 85, 250m^2 and 0.07μs, respectively.

. Ku band

From equations 62 and 66 the following equations are obtained when $[S_c/N_r] = 10$

$$4[R] - 2[\psi] - 233.0 = [\sigma] + [t] \qquad (86)$$

$$[R] + 50.3 = [\sigma] - [t] \qquad (87)$$

The values of σ and t obtained by solving these two simultaneous equations are given in Table III-21 for a 100 ft visibility fog.

TABLE III-21. OPTIMUM PULSE LENGTH AND MINIMUM REFLECTOR SIZE FOR Ku BAND IN 100 FT VISIBILITY FOG.

	Range (km)				
	1	2	4	10	20
[R]	30	33	36	40	43
4 [R]	120	132	144	160	172
-2 [ψ]	0.7	1.4	2.9	7.2	14.4
4 [R] - 2 [ψ]	120.7	133.6	146.9	167.2	186.4
4 [R] - 2 [ψ] - 233.0	-112.3	- 99.6	- 86.1	- 65.8	- 46.6
[R] + 50.3	80.3	83.3	86.3	90.3	93.3
2 [σ]	- 32.0	- 16.3	+ 0.2	+ 24.5	+ 46.7
2 [t]	-192.6	-182.9	-172.4	-156.1	-139.9
[σ]	- 16.0	- 8.2	+ 0.1	+ 12.3	+ 23.4
$\sigma(m^2)$	0.03	0.15	1.0	17	220
[t]	- 96.3	- 91.5	- 86.2	- 78.1	- 69.9
t (μs)	0.0002	0.0007	0.002	0.015	0.1

When a 'typical' attenuation is taken for 100 ft visibility fog, i.e., half the theoretical value, the effect this has on the optimum pulse length and reflector size is shown in Table III-22.

TABLE III-22. OPTIMUM PULSE LENGTH AND MINIMUM REFLECTOR SIZE FOR Ku BAND WITH "TYPICAL" ATTENUATION ASSUMED FOR 100 FT VISIBILITY FOG.

	Range (km)				
	1	2	4	10	20
$\sigma(m^2)$	0.002	0.14	0.9	11	95
t (μs)	0.0002	0.0007	0.005	0.01	0.05

. Ka band

When $[S_c/N_r] = 10$ and $[S_c/S_t] = 10$, substitution in equations 63 and 67 gives:

$$4[R] - 2[\psi] - 229.8 = [\sigma] + [t] \quad (88)$$

$$[R] + 47.0 = [\sigma] - [t] \quad (89)$$

Solving these equations for various values of R gives the following values for σ and t.

TABLE III-23. OPTIMUM PULSE LENGTH AND MINIMUM REFLECTOR SIZE FOR Ka BAND IN 100 FT VISIBILITY FOG.

	Range (km)				
	1	2	4	10	20
$-2[\psi]$	2.8	5.6	11.1	27.8	55.6
$4[R] - 2[\psi] - 229.8$	-107.0	- 94.2	- 74.7	- 42.0	- 2.2
$[R] + 47.0$	77.0	80.0	83.0	87.0	90.0
$2[\sigma]$	- 30.0	- 14.2	+ 8.3	+ 45.0	+ 87.8
$2[t]$	-184.0	-174.2	-157.7	-129.0	- 92.2
$\sigma(m^2)$	0.03	0.2	2.6	220	2500
t (μs)	0.0006	0.002	0.013	0.35	2.5

Assuming the 'typical' attenuation for 100 ft visibility fog, half the theoretical value, this optimum pulse length and reflector size are as listed below.

TABLE III-24. OPTIMUM PULSE LENGTH AND MINIMUM REFLECTOR SIZE FOR Ka BAND WITH "TYPICAL" ATTENUATION ASSUMED FOR 100 FT VISIBILITY FOG.

	Range (km)				
	1	2	4	10	20
$\sigma(m^2)$	0.03	0.15	1.4	46	1000
t (μs)	0.0005	0.001	0.007	0.07	1.0

. V band

The conditions for $[S_c/N_r] = 10$ and $[S_c/S_t] = 10$ is by substitution in Equations 64 and 68 as follows:

$$4[R] - 2[\psi] - 217.9 = [\sigma] + [t] \quad (90)$$

$$[R] + 44.0 = [\sigma] - [t] \quad (91)$$

Solving these equations gives the following values for σ and t.

TABLE III-25. OPTIMUM PULSE LENGTH AND MINIMUM REFLECTOR SIZE FOR V BAND IN 100 FT VISIBILITY FOG.

	Range (km)				
	1	2	4	10	20
$-2[\psi]$	10.0	20.5	40.9	102.4	204.8
$4[R] - 2[\psi] - 217.9$	- 87.9	- 65.4	- 33.0	+ 44.5	+158.9
$[R] + 44.0$	74.0	77.0	80.0	84.0	87.0
$2[\sigma]$	- 13.9	+ 11.6	+ 47.0	+128.5	+245.9
$2[t]$	-161.9	-142.4	-113.0	- 40.5	+ 71.9
$\sigma(m^2)$	0.2	3.8	220	2.7×10^6	2.0×10^{12}
t (μs)	0.008	0.08	2.2	9.3×10^3	4.0×10^9

With 'typical' attenuation figures for 100 ft visibility fog, the values for σ and t are as follows:

TABLE III-26. OPTIMUM PULSE LENGTH AND MINIMUM REFLECTOR SIZE FOR V BAND WITH "TYPICAL" ATTENUATION ASSUMED FOR 100 FT VISIBILITY FOG.

	Range (km)				
	1	2	4	10	20
$\sigma(m^2)$	0.1	1.2	21	4.7×10^3	1.5×10^7
t (μs)	0.005	0.02	0.2	29	3.4×10^4

6.12 Beacon Power

The signal received from a ground beacon, S_b, is given by the equation:

$$S_b = \frac{P_b G_b}{4\pi R^2} \cdot \frac{G \lambda^2}{4\pi} \cdot \psi \quad \text{watts} \tag{92}$$

where P_b = Beacon transmitter power

G_b = Beacon antenna gain

With typical beamwidths of 10° in azimuth and 10° in elevation, $G_b = 400$. Substituting this value, together with those given in Table III-11, the following equations for S_b, at the various frequency bands are obtained.

X band $[S_b] = 6.7 + [P_b] - 2[R] + [\psi]$ dBW (93)

Ku band $[S_b] = 7.3 + [P_b] - 2[R] + [\psi]$ dBW (94)

Ka band $[S_b] = 4.2 + [P_b] - 2[R] + [\psi]$ dBW (95)

V band $[S_b] = 1.3 + [P_b] - 2[R] + [\psi]$ dBW (96)

The above equations together with Equations 27 through 30 give the following values for S_b/N_r:

X band $[S_b/N_r] = 200.7 + [P_b] + [t] - 2[R] + [\psi]$ (97)

Ku band $[S_b/N_r] = 199.3 + [P_b] + [t] - 2[R] + [\psi]$ (98)

Ka band $[S_b/N_r] = 192.2 + [P_b] + [t] - 2[R] + [\psi]$ (99)

V band $[S_b/N_r] = 180.3 + [P_b] + [t] - 2[R] + [\psi]$ (100)

At a range of 10nm the beacon power required to give a signal to noise ratio of 10dB is given by the following equations.

X band $[P_b] = 10 - 200.7 - [t] + 85.4 - [\psi]$ (101)

$= -105.3 - [t] - [\psi]$ dBW

Ku band $[P_b] = -103.9 - [t] - [\psi]$ dBW (102)

Ka band $[P_b] = -96.8 - [t] - [\psi]$ dBW (103)

V band $[P_b] = -84.9 - [t] - [\psi]$ dBW (104)

Substituting values of ψ for various weather conditions gives the following values for the beacon transmitter power that produces a signal/noise ratio of 10dB at a range of 10nm.

TABLE III-27. BEACON POWER (mw) FOR A 10dB SIGNAL/NOISE RATIO AT 10 nm.

Frequency Band	Pulse Length	Rainfall Rates				Fog Densities	
	μs	0 mm/hr	1 mm/hr	4 mm/hr	16 mm/hr	400 ft	100 ft
X	1.0	0.029	0.031	0.036	0.09	0.032	0.044
	0.5	0.058	0.062	0.072	0.18	0.064	0.088
	0.1	0.29	0.31	0.36	0.90	0.32	0.44
Ku	1.0	0.04	0.055	0.12	8.1	0.055	0.19
	0.5	0.08	0.11	0.24	16.2	0.11	0.38
	0.1	0.4	0.55	1.2	81	0.55	1.9
Ka	1.0	0.21	0.76	21	6.6×10^{6}	0.66	84
	0.5	0.42	1.52	42	13.2×10^{6}	1.32	168
	0.1	2.1	7.6	210	6.6×10^{7}	6.6	840
V	1.0	3.2	100	1×10^{5}	1.2×10^{13}	65	5×10^{10}
	0.5	6.4	200	2×10^{5}	2.4×10^{13}	130	1×10^{11}
	0.1	32	10^{3}	1×10^{6}	1.2×10^{14}	650	5×10^{11}

6.13 Terrain Signal for a Pulse Width of 1 Microsecond

From Equations 21 through 24 and Table III-12, we obtain the following table which gives the values of $[S_t]$ for various ranges and weather conditions, with a transmitter pulse length of 1.0 μs.

TABLE III-28. TERRAIN SIGNAL (-dBw) VARIATION WITH RANGE

Frequency Band	Range km	Rainfall Rates				Fog Densities	
		0 mm/hr	1 mm/hr	4 mm/hr	16 mm/hr	400 ft	100 ft
X	1	61.7	61.72	61.8	62.22	61.74	61.9
	2	70.7	70.74	70.9	71.74	70.78	71.1
	4	79.7	79.78	80.1	81.78	74.86	80.5
	10	91.7	91.9	92.7	96.9	92.1	93.7
	20	100.7	101.1	102.7	111.1	101.5	104.7
Ku	1	58.7	58.84	59.2	61.26	58.86	59.42
	2	67.7	67.98	68.7	72.82	68.02	69.14
	4	76.7	77.26	78.7	87.94	77.34	79.58
	10	88.7	90.1	93.7	114.3	90.3	95.9
	20	97.7	100.5	107.7	148.9	100.9	112.1
Ka	1	62.1	61.8	63.2	69.34	61.74	63.98
	2	70.2	71.4	74.48	86.48	71.28	75.76
	4	79.2	81.6	87.76	111.76	81.36	90.32
	10	91.2	97.2	112.6	172.6	96.6	119.0
	20	100.2	112.2	143.0	263.0	111.0	155.8
V	1	67.1	68.7	71.9	81.7	68.54	77.34
	2	76.1	79.3	85.7	105.3	78.98	96.58
	4	85.1	91.5	104.3	143.5	90.86	126.06
	10	97.1	113.1	145.1	243.1	111.5	199.5
	20	106.1	138.1	202.1	398.1	134.9	310.9

6.14 Rain Signal for a Pulse Width of 1 Microsecond

From Equations 32 through 35 and the values of σ_u and ψ from Tables III-14 and III-12, the following table has been derived giving the values of $[S_r]$ for various ranges and weather conditions with a transmitter pulse length of 1.0 μs.

TABLE III-29. RAIN SIGNAL (-dBw) VARIATION WITH RANGE

Frequency Band	Range km	Rainfall Rates		
		1 mm/hr	4 mm/hr	16 mm/hr
X (Linear Polarization)	1	83.72	74.8	65.22
	2	89.74	80.9	71.74
	4	95.78	87.1	78.78
	10	103.9	95.7	89.9
	20	110.1	102.7	101.1
Ku (Circular Polarization)	1	87.74	79.1	73.16
	2	93.88	85.6	81.72
	4	100.16	92.6	92.84
	10	109.0	103.6	116.2
	20	116.4	114.6	147.8
Ka (Circular Polarization)	1	79.5	73.04	72.04
	2	86.1	81.18	86.18
	4	93.3	91.46	108.46
	10	104.9	112.3	165.3
	20	116.9	139.7	252.7
V (Circular Polarization)	1	75.4	69.6	73.4
	2	83.0	80.4	94.0
	4	92.2	96.0	129.2
	10	109.8	132.8	224.8
	20	131.8	186.8	376.8

6.15 Comment

The results obtained in this section are unified and summarized in Volume II of this report.

7.0 INTERFERENCE

7.1 Direct Interference

Direct interference arises when the signal received from another aircraft by direct transmission is greater than the desired signal from the ground within the operating range. The amplitude of the desired signal is always greater than 10dB above noise or 10dB above rain echo depending upon which is the greater. Since the most common cause for the limitation in range is the signal/noise ratio falling below 10dB, calculations are made of the conditions under which the interference is more than 10dB above the receiver noise level.

The amplitude of the interference signal, S_i, is given by the equation:

$$S_i = \frac{PG_1}{4\pi R^2} \quad \frac{G_2 \lambda^2}{4\pi} \quad \psi \qquad (105)$$

where G_1 = Antenna gain of the interfering radar in the direction of the interfered aircraft.

and G_2 = Antenna gain of the radar in the direction of the interfering aircraft.

A typical value for G_1 and G_2 is 1.0 when there is side lobe to side lobe transmission. Substituting this in Equation (105), together with the appropriate values for P and λ gives:

<u>X band</u> $[S_i] = -9.5 - 2[R] + [\psi]$ dBW (106)

<u>Ku band</u> $[S_i] = -13.4 - 2[R] + [\psi]$ dBW (107)

<u>Ka band</u> $[S_i] = -20.4 - 2[R] + [\psi]$ dBW (108)

<u>V band</u> $[S_i] = -29.3 - 2[R] + [\psi]$ dBW (109)

Combining these with Equations 27 through 30 of Section 6, gives the following values for [R], when $[S_i/N_r] = 10$dB.

X band $2[R] = 174.5 + [\psi] + [t]$ (110)

Ku band $2[R] = 168.6 + [\psi] + [t]$ (111)

Ka band $2[R] = 157.6 + [\psi] + [t]$ (112)

V band $2[R] = 139.7 + [\psi] + [t]$ (113)

Values of $2[R] - [\psi]$ are listed in the following table.

TABLE III-30. VALUES OF $2[R] - [\psi]$.

Frequency Band	R	2 [R]	Rainfall Rates				Fog Densities	
	km	dB	0 mm/hr	1 mm/hr	4 mm/hr	16 mm/hr	400 ft fog	100 ft fog
X	1	60	60	60.01	60.05	60.26	60.02	60.1
	10	80	80	80.1	80.5	82.6	80.2	81
	100	100	100	101	105	126	102	110
Ku	1	60	60	60.07	60.25	61.28	60.08	60.36
	10	80	80	80.7	82.5	92.8	80.8	83.6
	100	100	100	107	125	228	108	136
Ka	1	60	60	60.3	61.07	64.07	60.27	61.39
	10	80	80	83	90.7	120.7	82.7	93.9
	100	100	100	130	207	507	127	239
V	1	60	60	60.8	62.4	67.3	60.72	65.12
	10	80	80	88	104	153	87.2	131.2
	100	100	100	180	340	830	172	612

The above values are plotted on Figures III-38 to III-41, and from these curves Table III-31 is derived giving the range at which the interference signal is 10dB above noise.

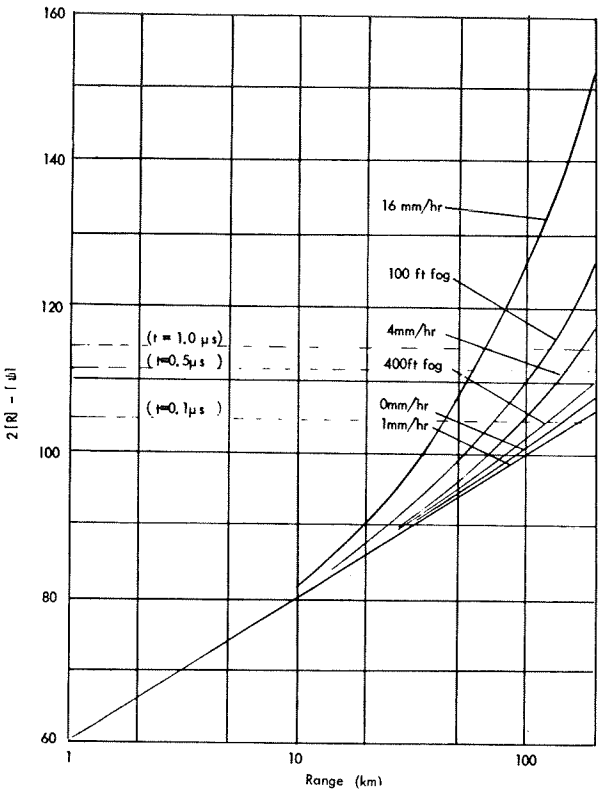

Figure III-38.
Values of 2 [R] - [ψ] for X band.

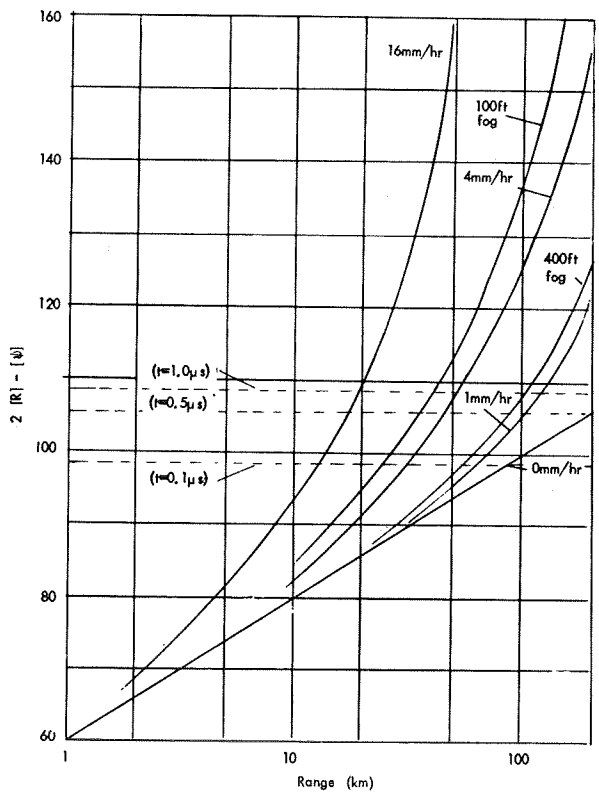

Figure III-39.
Values of 2 [R] - [ψ] for Ku band.

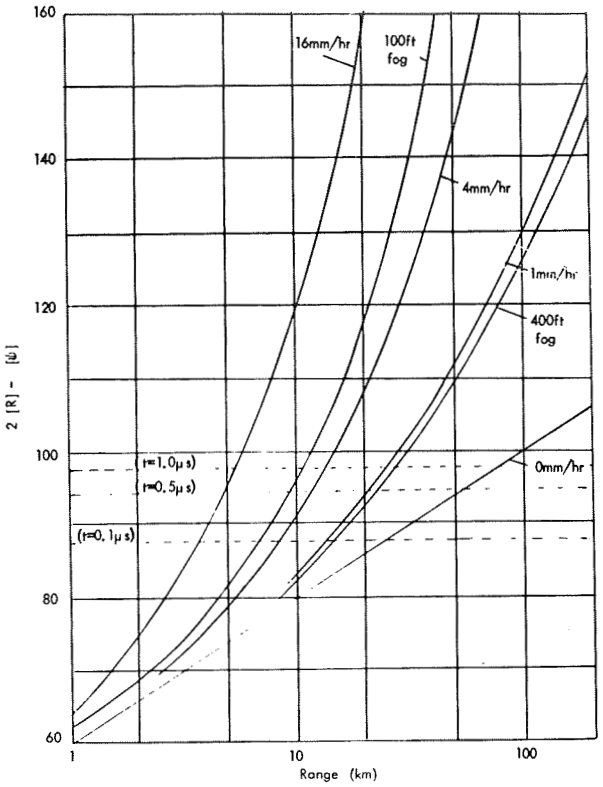

Figure III-40.
Values of 2 [R] - [ψ] for Ka band.

Figure III-41.
Values of 2 [R] - [ψ]for V band.

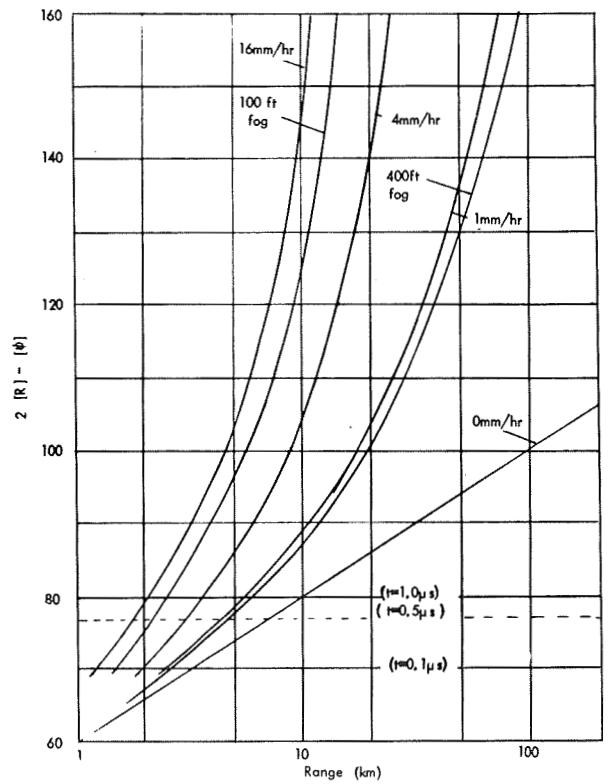

TABLE III-31. RANGE (km) AT WHICH DIRECT INTERFERENCE SIGNAL IS 10 dB ABOVE RECEIVER NOISE. SIDE LOBE TO SIDE LOBE TRANSMISSION

Frequency Band	Pulse Length μs	Rainfall Rates				Fog Densities	
		0 mm/hr	1 mm/hr	4 mm/hr	16 mm/hr	400 ft fog	100 ft fog
X	1.0	500	340	170	64	250	120
	0.5	360	270	150	60	210	110
	0.1	160	120	100	44	120	70
Ku	1.0	250	110	52	19	110	42
	0.5	180	100	46	17	90	36
	0.1	80	60	32	13	55	26
Ka	1.0	76	25	14	5.4	28	11
	0.5	53	21	12	4.8	23	10
	0.1	24	14	8.2	3.6	15	7
	1.0	10	5.5	3.8	2.1	5.9	2.4
V	0.5	7.0	4.3	3.1	1.8	4.5	2.1
	0.1	3.2	2.3	2.0	1.2	2.5	1.4

When one of the beams is pointing in the direction of the other aircraft, there is a large increase in the amplitude of the interference signal. For example, with the Ku band radar

G_1 becomes 37.7 and Equation 107 becomes

$$[S_i] = 24.3 - 2[R] + [\psi] \text{ dBW} \qquad (114)$$

and the range at which $S_i/N_r = 10$dB is given by the equation,

$$2[R] = 204 + [\psi] + [t] \qquad (115)$$

Similarly, when both antennas are pointing at each other

$$2[R] = 241.7 + [\psi] + [t] \qquad (116)$$

The values of R that satisfy Equations 115 and 116 are listed in Table III-32.

TABLE III-32. RANGE (km) FOR INTERFERENCE SIGNAL TO BE 10dB ABOVE RECEIVER NOISE WITH THE Ku BAND RADAR.

	Pulse Length μs	Rainfall Rates				Fog Densities	
		0 mm/hr	1 mm/hr	4 mm/hr	16 mm/hr	400 ft fog	100 ft fog
One beam	1.0	1000	360	160	42	300	115
pointing at	0.5	1000	340	150	40	280	110
other aircraft	0.1	1000	290	130	36	240	94
Both beams	1.0	1000	700	310	66	540	200
pointing at	0.5	1000	640	290	64	510	190
other aircraft	0.1	1000	580	260	59	460	180

7.2 Reflected Interference

When aircraft are placed as shown in Figure III-42, Aircraft (2) receives a signal S_t, from its own radar reflected from the ground, and also an interference signal, S_i, from aircraft (1) reflected from the ground. The amplitude of S_t is given by the equation:

$$S_t = \frac{PG}{4\pi R_2^2} \gamma \beta \frac{tc}{2} \frac{\tan\theta}{4\pi R_2} \frac{G\lambda^2}{4\pi} \psi_2^2 \qquad (117)$$

The amplitude of S_i is given by the Equation:

$$S_i = \frac{PG}{4\pi R_1^2} \gamma \beta R_1 \frac{tc}{2} \frac{\tan\theta}{4\pi R_2^2} \frac{G\lambda^2}{4\pi} \psi_1 \psi_2 \qquad (118)$$

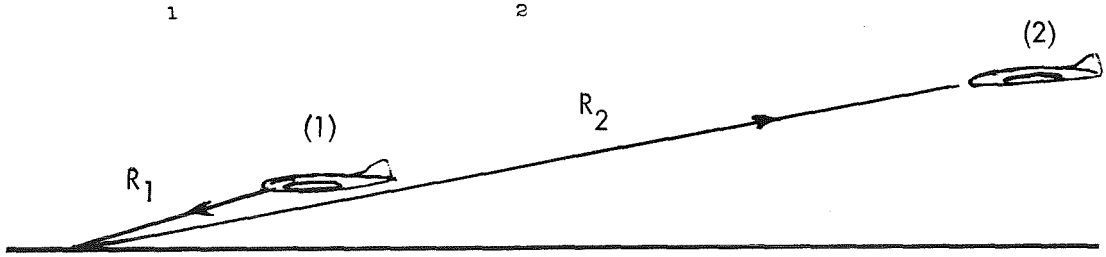

Figure III-42. Reflected Interference

where ψ_1 = Attenuation along path R_1

ψ_2 = Attenuation along path R_2

The ratio S_i / S_t is $\dfrac{R_2}{R_1} \quad \dfrac{\psi_1}{\psi_2}$

Expressed in dBs,

$$[S_i / S_t] = [R_2] - [R_1] + [\psi_1] - [\psi_2] \qquad (119)$$

Maximum interferences occur when R_1 has its minimum value, i.e. just before the aircraft rolls out. With a typical value for R_1 of 200m, the ratio of $[S_i / S_t]$ for various ranges and weather conditions is listed in the following table.

TABLE III-33. RATIO OF REFLECTED INTERFERENCE TO TERRAIN SIGNAL.

Frequency Band	R km	Rainfall Rates 0 mm/hr	1 mm/hr	4 mm/hr	16 mm/hr	Fog Densities 400 ft fog	100 ft fog
X	1	7	6.99	6.95	6.74	6.48	6.90
	2	10	9.98	9.90	9.48	9.96	9.80
	10	17	16.9	16.5	14.4	16.8	16.0
	20	20	19.8	19.0	14.8	19.6	18.0
Ku	1	7	6.93	6.75	5.72	6.92	6.64
	2	10	9.86	9.50	7.44	9.84	9.28
	10	17	16.3	14.5	4.20	17.2	13.4
	20	20	18.6	15.0	- 5.6	18.4	12.8
Ka	1	7	6.70	5.93	2.93	6.73	5.61
	2	10	9.40	7.86	1.86	9.46	7.22
	10	17	14.0	6.30	-23.7	14.3	3.1
	20	20	14.0	-1.40	-61.4	14.6	-7.8
V	1	7	6.20	4.60	- 0.30	6.28	1.88
	2	10	8.41	5.20	- 4.60	8.56	-0.24
	10	17	9.00	-7.00	-56.0	2.60	-34.2
	20	20	4.00	-24.0	-126	5.6	-82.4

REFERENCES

1. Cosgriff, R.L., Peaks, W.H. and Taylor, R.C., "Electromagnetic Reflection Properties of Natural Surfaces With Applications to Design of Radars and Other Sensors" (Terrain Handbook). The Ohio State University Research Foundation, February 1959.

2. Kranson, H. and Randig, G., "Terrain Backscattering Characteristics at Low Grazing Angles For X-and S-Band". Technical Note, IEEE Proceedings, December 1966.

3. Katz, I. and Spetner, L.M., "Polarization and Depression - Angle Dependence of Radar Terrain Return". J. Res. NBS, Vol. 64D, September - October 1960.

4. Taylor, R.C., "Terrain Return Measurements at X, Ku and Ka Band", IRE National Convention Record, Vol. 7, Pr. I, pp. 19-26, 1959.

5. Kerr, D.E., "Propagation of Short Radio Waves", McGraw - Hill, New York, 1951.

6. Medhurst, R.G., "Rainfall Attenuation of Centimeter Waves: Comparison of Theory and Measurement", IEEE Transactions on Antennas and Propagation, July 1965, pp. 550-564.

7. Hawkins, H.E. and LaPlant, O., "Radar Performance Degradation in Fog and Rain", IRE Transactions on Aeronautical and Navigational Electronics, March 1959. pp. 26-30.

8. Gunn, K.L.S. and East, T.W.R., "The Microwave Properties of Precipitation Particles", Quarterly Journal Royal Meteorology Society, Volume 80, pp. 522-545, October 1954.

9. Panasiewicz, J.J., "Enhancement of Aircraft Radar Return by Use of Airborne Reflectors and Circular Polarization", IEE Conu. Record, Volume 4, pt. 8, pp. 89-96, 1956.

10. McFee, R. and Maher, T.M., "Effect of Surface Reflections on Ram Cancellation of Circularly Polarized Radars", IRE Transaction on Antennas and Propagation April 1959, pp. 199-201.

DISTRIBUTION LIST

NASA - Electronics Research Center
55 Broadway
Cambridge, Mass. 02139

Attention:	Robert W. Wedan	Code: P	1
	Dr. Gene G. Mannella	Code: T	1
	William J. Raine	Code: PH	1
	Leo M. Keane	Code: PS	1
	Ronald J. Madigan	Code: PHD	1
	Harold D. Decker	Code: PHD	10
	Janis Vilcans	Code: PHD	1
	Joseph A. LoVecchio	Code: PHD	1
	Richard J. Miner	Code: PHD	1
	John C. Loria	Code: PHD	1
	William J. O'Keefe	Code: PHD	1
	Robert A. Woolson	Code: ANP	11
	Dr. Robert J. Mailloux	Code: ROI	1
	Francis J. Larussa	Code: TII	1

NASA - Ames Research Center
Moffett Field
California 94035

Attention:	Norman S. Johnson	Code: FS	1
	John DiMeff	Code: FI	1
	Ron Hruby	Code: FI	1

NASA - Headquarters
OART
Washington, D.C. 20546

Attention:	Albert J. Evans	Code: RA	1
	Charles Gould	Code: RES	1
	Frank J. Sullivan	Code: RE	1

NASA - Langley Research Center
Langley Station
Hampton, Virginia 23365

Attention:	G.B. Graves	Code: 15.00	1

Federal Aviation Agency
800 Independence Avenue
Washington, D.C. 20590

Attention:	James H. Muncy	Code: RD-2	1
	Jack P. Stell	Code: SS-1	1
	James Thompson	Code: SS-2	1

AFSC - Special Technical Liaison Office
Massachusetts Institute of Technology
68 Albany Street
Cambridge, Mass. 02139

Attention: Capt. Mark R. Jensan 1

Eastern Airlines
10 Rockefeller Plaza
New York, N.Y. 10020

Attention: Mr. S. L. Higginbottom 1

Braniff International
P. O. Box 35001
Dallas, Texas 75235

Attention: Mr. Dan Hughes

Northeast Airlines
239 Prescott Street
East Boston, Mass. 02128

Attention: Mr. J. E. White 1

McDonnell - Douglas Corporation
P. O. Box 516
St. Louis, Missouri 63166

Attention: McDonnell Library, Dept. 213 1

The Boeing Company
Box 3733
Seattle, Washington

Attention: Mr. Mel Abbott 4C-37 1

Lockheed California Company
Building 90
Thornton & Ontario Streets
Burbank, California

Attention: Dr. Edward H. Marcard 1
Mr. Maurice Franco 1

Singer - General Precision Inc.
Kearfott Division
1150 McBride Avenue
Little Falls, N.J. 07424

Attention: Myron Rosenthal 1

Norden Division
United Aircraft Corporation
110 Helen Street
Norwalk, Conn.

Attention: Dr. Lester Kosowsky 1

DISTRIBUTION LIST (cont'd)

United States Air Force - AFSC
Systems Engineering Group - RTD
Wright Patterson Air Force Base
Dayton, Ohio

Attention: R. J. Harnett Code: SEKRA 1

USAF Flight Dynamics Laboratory
Wright Patterson Air Force Base
Dayton, Ohio

Attention: Mr. George Yingling 1

Naval Air Systems Command
Washington, D.C. 20360

Attention: AIR 5333 1

Commanding General
U.S. Army Electronics Command
Fort Monmouth, N.J. 07728

Attention: AMSEL-VL-N (Mr. Joseph Saganowich) 1

United Airlines
4085 Prudential Center
Boston, Mass. 02199

Attention: Mr. F. Paul Weiss 1

Pan American Airways
Hangar 14
John F. Kennedy International Airport
Jamaica, N.Y. 11430

Attention: Mr. Thomas Flanagan 1

Trans World Airlines
Overland Base
Kansas City International Airport
Kansas City, Missouri 64153

Attention: Mr. R. A. Arrington 1

Maxson Electronics
Great River
New York

Attention: Mr. James Anania 1

Texas Instruments
400 Totten Pond Road
Waltham, Mass. 02154

Attention: Dr. Conrad Rauch 1

Air Transport Association
1000 Connecticut Avenue, N.W.
Washington, D.C.

Attention: S. Poritzky 1

Air Line Pilots Association
1329 E Street, N.W.
Washington, D.C. 20004

Attention: Ted Linnert 1

American Airlines
633 Third Avenue
New York, N.Y. 10017

Attention: Mr. S. L. Seltzer 1
Mr. Robert K. Ransone 1

American Airlines Maintenance & Engineering Center
Tulsa, Oklahoma 74151

Attention: Mr. Robert Rogers 1

American Airlines
Laguardia Airport Station
Flushing, N. Y. 11371

Attention: Mr. Paul Miller 1

United Airlines
Executive Offices
P. O. Box 66100
Chicago, Ill. 60666

Attention: Mr. Marvin Whitlock 1
Mr. H. J. Reid 1